WSRC-TR-2001-00211

KEYWORD:
Salt Waste Processing Facility (SWPF),
Tetraphenylborate,
Cesium

Retention Period: Permanent

Demonstration of Small Tank Tetraphenylborate Precipitation Process Using Savannah River Site High Level Waste

T. B. Peters
M. J. Barnes
F. F. Fondeur
S. D. Fink
R. W. Blessing
R. E. Norcia
J. G. Firth
C. W. Kennell
T. R. Tipton
B. B. Anderson

Publication Date: May 31, 2001

Westinghouse
Savannah River Company
Aiken, SC 29808

This document was prepared in conjunction with work accomplished under Contract No. DE-AC09-96SR18500 with the U.S. Department of Energy.

DISCLAIMER

Demonstration of Small Tank Tetraphenylborate Precipitation Process using Savannah River Site High Level Waste

AUTHORS

T. B. Peters, Waste Processing Technology Date

M. J. Barnes, Waste Processing Technology Date

F. F. Fondeur, Waste Processing Technology Date

R. Norcia, Process Control Engineering Date

C. Q. Nichols, Process Control Engineering Date

J. G. Firth, Process Control Engineering Date

C. W. Kennell, Process Control Engineering Date

T. R. Tipton, Process Control Engineering Date

B. B. Anderson, Analytical Development Section Date

DESIGN CHECK

R. C. Fowler, Process Engineering Date
(per Manual E7, Procedure 2.40)

APPROVALS/REVIEW

S. D. Fink, Manager, Liquid Waste Processing Technology Date

J. F. Walker, TFA System Lead	Date
R. E. Edwards, Manager, Process Engineering	Date
J. T. Carter, SWPF Director of Engineering	Date
W. L. Tamosaitis, Manager, Waste Processing Technology	Date

ABBREVIATIONS

AA	Atomic Absorption
ADS	Analytical Development Section
CSTR	Continuously stirred tank reactor
DF	Decontamination Factor
HLW	High Level Waste
HPLC	High Performance Liquid Chromatography
ICP-ES	Inductively-coupled plasma emissions spectroscopy
ICP-MS	Inductively-coupled plasma mass spectroscopy
IIT B-52	Acronym for antifoam reagent designed by researchers from the Illinois Institute of Technology (IIT)
MST	Monosodium titanate
NaTPB	Sodium tetraphenylborate
PuTTA	Plutonium triphenyltrifluoroacetone scintillation analysis
3PB	Triphenylboron
2PB	Diphenylborinic acid
1PB	Phenylboronic acid
SRS	Savannah River Site
SRTC	Savannah River Technology Center
STTP	Small Tank Tetraphenylborate Precipitation
TPB	Tetraphenylborate
TR&C	Task Requirements and Criteria
WPT	Waste Processing Technology

1.0 EXECUTIVE SUMMARY

This report details the experimental effort to demonstrate the continuous precipitation of cesium from Savannah River Site High Level Waste using sodium tetraphenylborate. In addition, the experiments examined the removal of strontium and various actinides through addition of monosodium titanate. To prevent any adverse foaming, personnel added a chemical additive, designated as IIT B-52, developed by researchers at the Illinois Institute of Technology. The waste used in the experiments represents a mixture from a number of tanks at the site and includes as part of the material the same source waste as used in an earlier demonstration of the process that exhibited poor hydraulics due to foaming.

The process demonstration met all objectives:

- The experiment demonstrated successful removal of cesium from the waste. This waste required a decontamination factor (DF) of 10,000. During the entire experiment, the decontamination factor averaged 1.4 million after the equipment reached steady-state operation, including elevated temperature operations.

- The monosodium titanate successfully removed the actinides (Pu, U) from solution yielding a solution with an average alpha dose below 0.214 nCi/g after treatment versus a process requirement of 18 nCi/g.

- The experiment demonstrated successful removal of strontium from the waste. This waste required a target DF of 19.3 to meet Saltstone requirements. During the entire experiment, the decontamination factor averaged 45.6 after the equipment reached steady-state operation.

- Throughout the duration of the testing we observed little, if any evidence of foaming. We observed some minor frothing in the sample lines before reaching 45 °C, and the interstage overflow tube between CSTR#1 and CSTR#2 plugged after 71 hours of operation.

- The slurry showed evidence of catalytic decomposition of the tetraphenylborate during the testing at 45 °C, giving a calculated benzene generation rate of 2.4 mg/(L•h).

2.0 INTRODUCTION

In 1995, batch processing of tetraphenylborate in Tank 48H started.[1] However, extensive production of benzene during processing led to the cessation of operations. Subsequent

evaluations identified the need for a more robust safety envelope using a small, continuous process.[1] A previous demonstration of the operation of the precipitation reaction with material from the Savannah River Site (SRS) tank farm in a continuous fashion occurred in 1999, but failed to achieve steady-state performance due to extensive foaming.[3] The Alt-Salt project management requested that the Savannah River Technology Center (SRTC) "conduct additional tests using real waste containing the recommended chemical additive to demonstrate sustained decontamination of waste, balanced hydraulics, and reduced foaming".[4] This report provides the details of those experiments.

3.0 EXPERIMENTAL

The experiments used custom designed equipment to examine the chemical process for the continuous precipitation operation of the proposed process. The work did not include filtration of the product slurry or recycle of any process streams as will occur in the proposed process. The experiments occurred in remote cells using manipulators to control manual operations and computer driven process control.

3.1 Equipment

Fabrication and assembly of the equipment and control racks required the coordinated efforts of a number of organizations at SRS, including personnel from SRTC, Construction, Process and Controls Technology, Equipment Engineering Section, Thermal Fluids Labs, and the Shielded Cells Operators.

3.1.1 The Feed Tank Rack

The Feed Tank Rack holds two, 4 L feed bottles and allows monitoring of the mass of the contents through the use of load cells. Each load cell (Inotek, HPSM-D3-6KG-10P9) has a 6 kg limit. The design ensures that only the weight of the bottle and the feed solutions register on the load cells; all other penetrations into the bottle do not contact any part of the bottle. Each feed bottle includes a funnel to allow refilling during the experiment. The design provides tubing, with intake points near the bottom of the bottles, to facilitate pumping the contents from each feed. A Heidolph RZR 2041 variable speed overhead stirrer agitates the contents of each feed bottle. The rotational speed of the stirrer is displayed through the LCD panel on the stirrer and is also confirmed through the use of a Dart Controls PU-20E Hall Effect sensor on each stirrer. This rack has a footprint of about 2 x 2 feet.

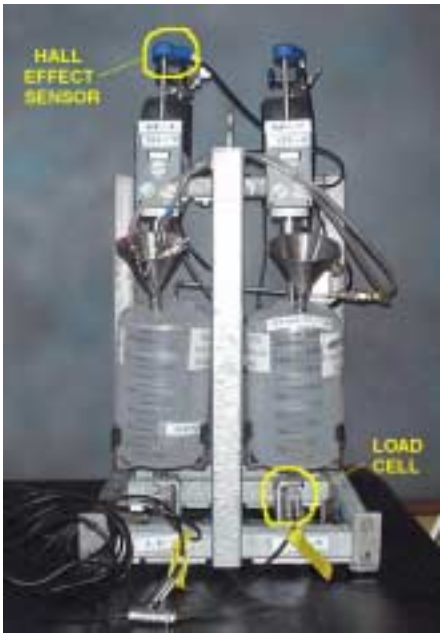

Figure 1. Feed Tank Rack.

3.1.2 The Main Rack

The main rack (3' by 2' footprint) contains the two Continuous Stirred Tank Reactors (CSTRs). (Figure 2). Each reactor has a 1 L working volume, including the effect of the internal devices such as the cooling coils, baffles and draw tubes. The design mounts each reactor on a 6 kg-limited load cell (Inotek, HPSM-D3-6KG-10P9) to monitor the weight of the vessel contents; penetrations into the vessel do not contact the reactor. In addition, each reactor has the same stirring design as the feed bottles, including an overhead stirrer and Hall Effect sensor setup (Heidolph RZR 2041 and Dart Controls PU-20E, respectively). Four small variable speed piston pumps and pump heads from FMI, Inc.(QVG50 and Q0(SSY) respectively) provided feed flow and backup flow capacity. Nitrogen enters a penetration at the top of the reactor. Experiments with simulated waste demonstrated that the available nitrogen flow did not ensure anoxic conditions in the reactors. Hence, personnel altered the design to include a shroud (Figure 3) designed to fit around the top of the reactor and the pipe anchor. An additional nitrogen line enters into the shroud, and proved successful in keeping oxygen levels below 4.5% during the experiments with simulated waste. A dual-syringe pump (KD Scientific model #101) mounted on top of the rack provided the antifoam flow to each reactor Rheotherms (thermal loss flow meters, INTEK, 111D-I-TU1/16[1/4E][SS]-4/20) precisely monitored the flows from the pumps. CSTR#1 overflows into CSTR#2 and CSTR#2 overflows into the Product Receipt Rack (see 3.1.3, below) using gravity-driven, open-channel flow. In the case of a plug in either overflow, two fluid metering pumps provide an alternate

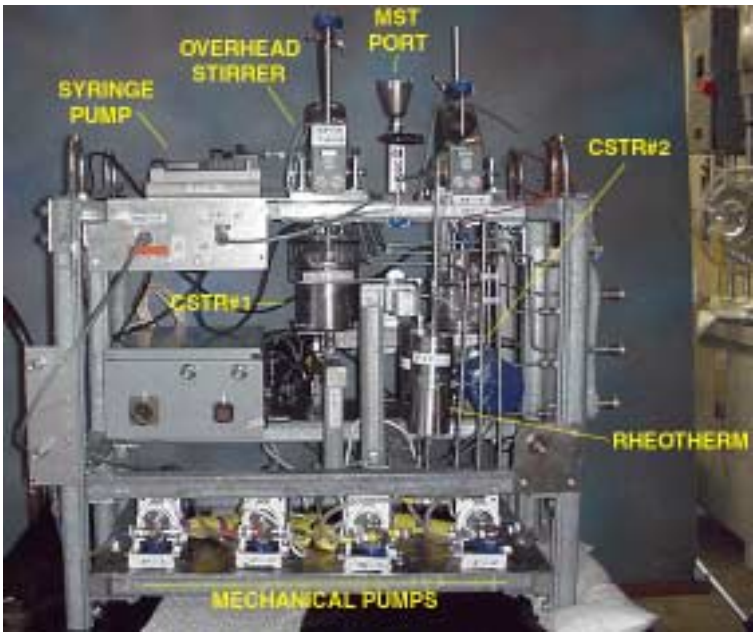

Figure 2. Vessel Rack.

Figure 3. The CSTR Shroud.

means to maintain the desired operating liquid level. Finally, personnel added MST through a funnel on top of the rack (personnel modified the design to include the funnel after testing with simulated waste showed that adding MST via one of the feed bottles led to settling in the feed lines).

3.1.3 The Product Receipt Rack

The Product Receipt Rack houses the receipt carboy and the sample port valve. A 60kg-limited load cell (Inotek, HPSM-D3-60KG-10P9) monitors the weight of the carboy and its contents. Again, the design ensures the downcomer into the carboy does not touch the vessel. A spout on the bottom facilitates drainage of the contents. The funnel on the top allows addition of water to flush the sampling valve or the vessel.

Figure 4. Product Receipt Rack

3.1.4 The Heating/Cooling System

The experiment required temperature control. The design includes one heater/chiller unit for each reactor. The circulating fluid (water) passes through suspended coils in each reactor. Given the required temperatures (25 °C and 45 °C), the design used two VWRbrand Heated/Refrigerated Circulators, Model# 1167, which had 300 W cooling and 1000W of heating capacity.

3.1.5 The Overall System

The design provides for separate assembly and entry of each rack into the shielded cells. Once positioned in the cell, personnel connected the three racks to each other and the chillers (Figures 6 and 7). The connected apparatus filled the entire width of the cell plus the raised margins between the surrounding cells. Including the connections to the controller rack, the design includes a total of 18 connections (gas, water or electrical) made by the cells operators.

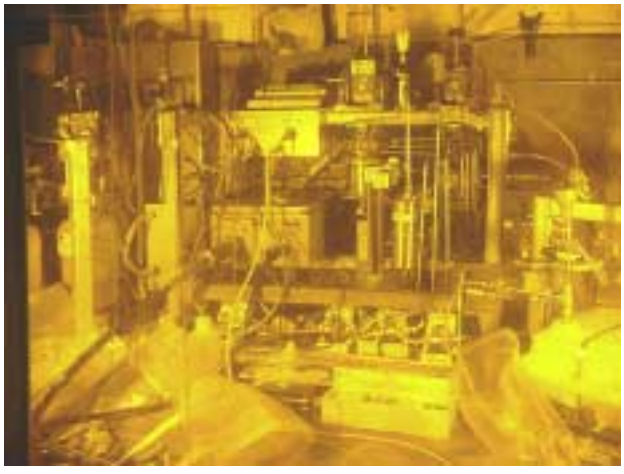

Figure 6. The Assembled Apparatus

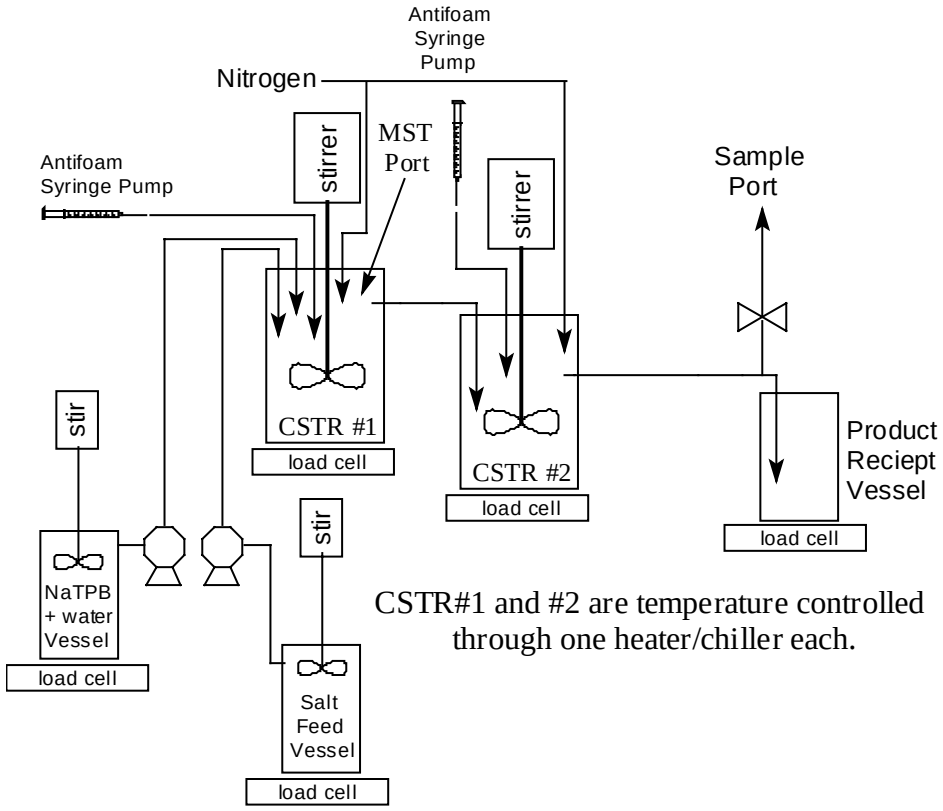

Figure 7. Diagram of the Assembled Apparatus.

3.1.6 The Control Rack

Most of the equipment on the inside racks was either controlled or monitored through an instrument controller on the outside of the cells. The instrument controller is a typical Windows NT™ computer (Pentium-3/866 MHz) and uses the FIX32™ software package for communication to the equipment. An instrument controller located outside of the cells either controlled or monitored most of the equipment. The control and monitoring functions occurs via two large cables equipped with a 19 pin and 55 bulkhead connector. Two thermocouple cables and several gas

Figure 8. Process Control Rack.

lines also run from the control rack to the equipment racks. The instrument controller operated the following equipment.

- 2 heater/chillers
- 4 fluid metering pumps
- 2 nitrogen flowmeters to the reactors

The controller monitored the following equipment.

- 2 load cells for the feed bottles
- 2 stirrers for the feed bottles
- 2 load cells for the reactors
- 2 stirrers for the reactors
- 1 load cell for the receipt vessel

The instrument controller records all the data on the hard drive. Using the FIX32™ program, one can graph or display all the data to examine for trends.

3.2 Exploratory Measurements – Foam Control

A previous demonstration of the operation of the precipitation reaction with material from the Savannah River Site (SRS) tank farm in a continuous fashion occurred in 1999, but failed to achieve steady-state performance due to extensive foaming.[3] The project management requested that the Savannah River Technology Center (SRTC) "conduct additional tests using real waste containing the recommended chemical additive to demonstrate sustained decontamination of waste, balanced hydraulics, and reduced foaming".[4] To prevent any adverse foaming during the operation of this experiment, personnel added a chemical additive, designated as IIT B-52, developed by researchers at the Illinois Institute of Technology. This material is designed to act both as an antifoam and a defoamer.
While previous tests [7] show that the B-52 works well with simulated waste to prevent adverse foaming, this study represents the first test with high-level waste.[5]
Personnel performed two different antifoam experiments to determine if real waste would undermine the ability of B-52 to prevent adverse foaming.

3.2.1 The First Antifoam Test

The first antifoam test used rapid stirring of high level waste slurry to determine antifoam efficacy. Personnel used 210 mL of real waste salt solution (see Table 1 for composition). This was added to 250 mL of a NaTPB/dilution water/MST (MST from AquAir, 21.1 wt. %) mixture

to generate a 4 wt % TPB slurry that containing 4.7 M sodium. Personnel placed the slurry in a 1000 mL plastic beaker and stirred

Table 1. Important Components of the Real Waste Salt Solution †

Analysis For	Result	Analysis	Result
Cesium	0.000814 M	Mercury	• 5E-08 M
Sodium	10.3 M	gamma scan	8.15E+09 dpm/mL
Potassium	0.0873 M	Nitrate (NO_3^-)	0.0191 M
^{90}Sr	5.57E+06 dpm/mL	Nitrite (NO_2^-)	0.0155 M
$^{238}Pu + {}^{239/240}Pu$	1140 dpm/mL	Sulfate (SO_4^{2-})	• 0.000521 M
$^{238}U + {}^{235}U$	3.84 mg/L	Hydroxide (HO^-)	6.19 M

at 500 rpm for 1/2 hour (left photo in Figure 9), using the same impellors as the previous Barnes test.[13] Since no adverse foaming occurred, we increased the agitator speed to 1000 rpm for 1/2 hour (right picture in Figure 9). Personnel then transferred the slurry to a new 1000-mL plastic beaker that contained enough antifoam to yield ~100 ppm of antifoam in the final slurry. We stirred this mixture at 500 rpm (left photo in Figure 10)for 1/2 hour. As with the case with

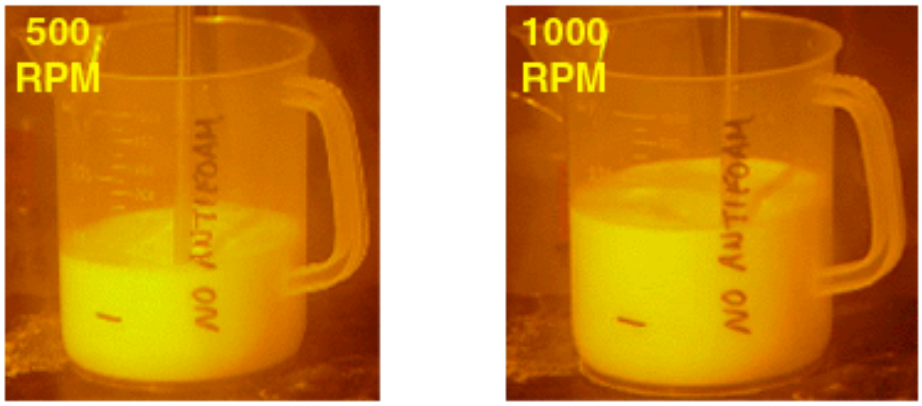

Figure 9. 500 RPM, and 1000 rpm Stirring Respectively, No Antifoam

no antifoam, we noted little foaming. We then stirred the mixture at 1000 for 1/2 hour (right photo in Figure 10) and again, observed little evidence of foaming.

As an additional check, personnel archived the slurry and two weeks later, repeated the test by stirring the slurry at 1000 rpm for 1/2 hour; to determine if antifoam decomposition could lead to

† A total of 8L of real waste salt solution was used in the STTP Demo, of which a ~6L volume was from Tank 37H, a ~1.5L volume was from Tank 44F, and a ~0.5 L volume was from a multi-tank composite which itself was a composite of Tanks 13H, 29H, 30H, 32H, 34H, 35H, 36H, 38H, 39H, 41H, and 43H.

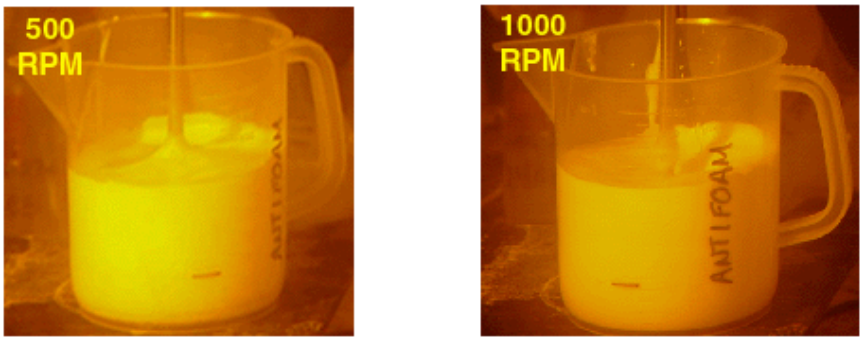

Figure 10. 500 rpm, and 1000 rpm Stirring Respectively, With Antifoam.

unfavorable foaming. During stirring, we did not observe any serious foaming (Figure 11). This finding suggests the possibility that even the decomposition products of the B-52 antifoam may prove effective antifoaming agents.[11] After this last stirring test, personnel archived the slurry

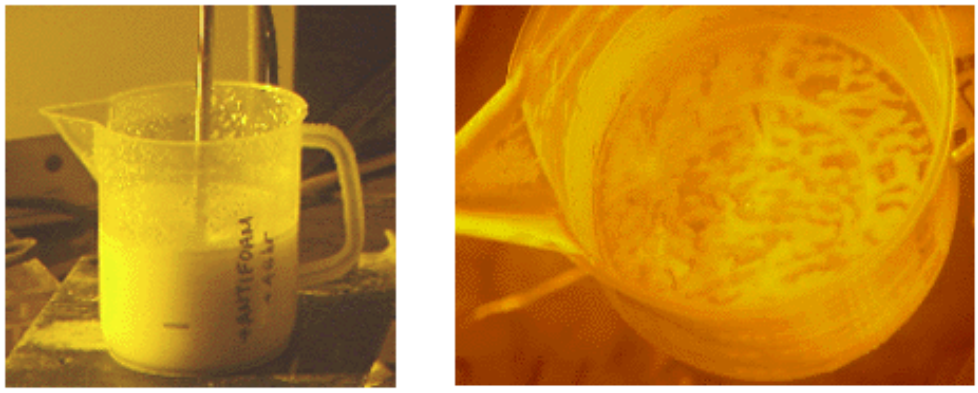

Figure 11. 1000 rpm Stirring After Two Weeks

and Figure 11 shows the residue left in the beaker after pouring the slurry. The beaker contained MST/TPB solids, but no visibly apparent oils or organic layers.

3.2.2. The Second Antifoam Test

The second antifoam test more closely mimicked previous antifoam tests using simulated waste, [7, 12] and used a large graduated glass column. The nominal 2L column included a fritted disk in the bottom. The column also included a gas inlet port below the fritted disk and a drain port above the disk (Figure 12). The first part of this test measured the foaming of the salt solution alone (i.e., no added NaTPB).

Figure 12. The Antifoam Column

By passing a moderate 200 mL/min of nitrogen through the viscous salt solution, a foamy, effervescent solution formed that filled ~2x the original volume (Figure 13 - the point on the column marked "B").

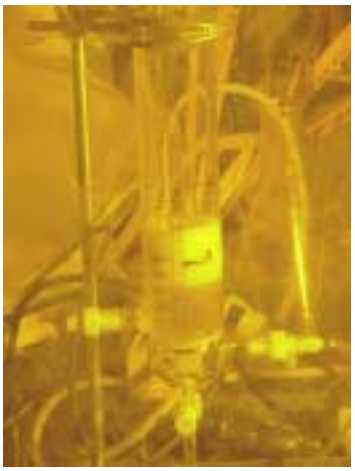

Figure 13. Salt Solution Foaming

After the salt solution settled, personnel added the NaTPB/dilution water/MST solution to the column, generating a slurry. Nitrogen flowed through the column at 200 mL/min for 2 minutes to mix the contents. By the end of that time, the slurry foam expanded to ~2.75x the original height (left photo in Figure 14). After 1/2 hour the foam did not settle to any appreciable degree.

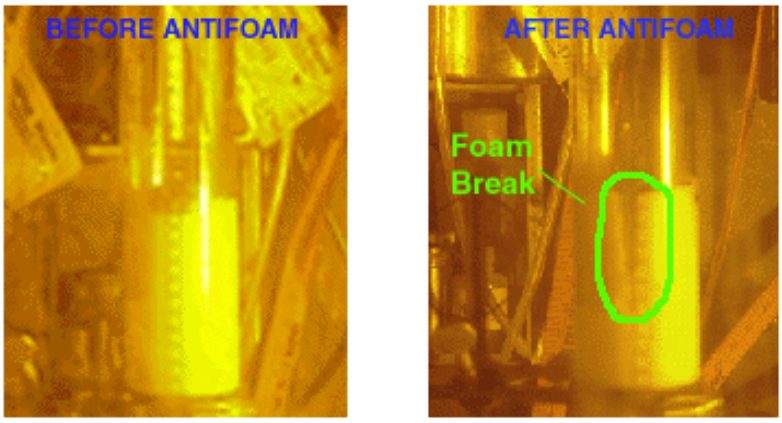

Figure 14. Initial Slurry Foaming and Antifoam Addition

The researchers decided to add a small amount of antifoam solution; enough to generate an even distribution of 75 ppm concentration of the antifoam. After about 10 minutes personnel noted a slight breaking of the foam (right photo in Figure 14), and this was likely due only to the added liquid. The foam did not collapse any more during the next hour. At that time, personnel added antifoam sufficient to raise the antifoam concentration to 500 ppm if well mixed in the bulk slurry. After a few minutes, the foam began to appreciably collapse (Figure 15). Allowing a small amount of gas into the column accelerated the foam breakup.

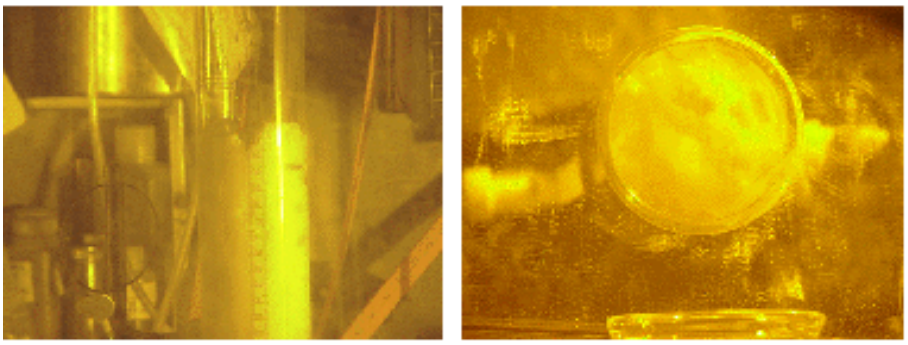

Figure 15. Foaming After adding 500 ppm of Antifoam

Adding another 500 ppm of antifoam (sufficient to reach a cumulative concentration of 1000 ppm in the well mixed slurry) solution accelerated the collapse of the foam (Figure 16).

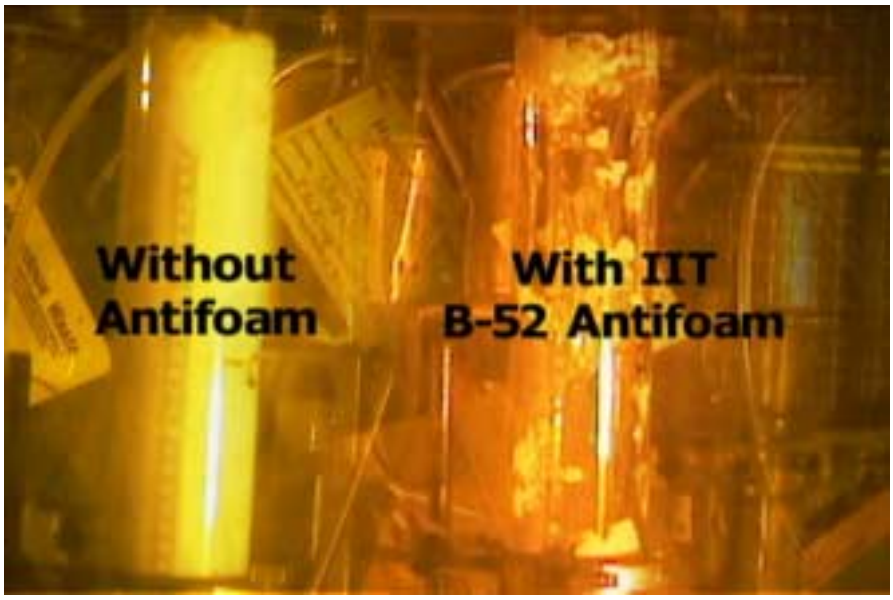

Figure 16. Foam Before and After adding 1000 ppm of Antifoam

In summation, the real waste/TPB slurries will foam when actively purged with gas (column test), but not to any significant extent when simply agitating at prototypical conditions (i.e., stirring test). When the slurry does foam, the B-52 antifoam provides a good defoaming capability even when applied in a non-ideal manner (adding to the top of a column of foam instead of having a constant delivery into the solution).

3.3 Exploratory Measurements – Oxygen Control

The authors utilized the Ocean Optics FOXY™ fiber optic oxygen sensor and newest version of the OOISensors™ software to record oxygen content as a function of time. The testing examined the effectiveness of the nitrogen headspace purge used to reduce and maintain an oxygen concentration below 4.5 vol % in the headspace of the CSTR above the liquid. Personnel purged the vessel with a maximum flow rate of 30 cc/min of ultra-high-purity nitrogen. The second CSTR proved more amenable to the placement of a small fiber optic probe due to the large area above the top and below the supporting mandrel, which served to secure the various feed and service tubes. Therefore, all measurements occurred in the headspace or liquid volume of the second CSTR. Personnel calibrated the oxygen sensor in air and nitrogen prior to each introduction into the CSTR headspace. Based on previous calibrations,[10] we made the assumption that the calibration would not change significantly (2-3%) if we calibrated the probe in gas and then introduced into liquid. Data from several tests exhibited drift of the oxygen measurements, and the presence of a bright halogen lamp behind the rig complicated that calibration in some instances, introducing a 3-4% bias over the course of the experiment. The data presented here provide a measure of the effectiveness of the purge, and the discussion describes the steps taken to identify appropriate purge geometry and flow rates after subsequent measurements indicated inadequate purge. Appendix 1 contains a more detailed description of the oxygen monitoring procedure.

Figure 17 displays the measurements for the final configuration after modifications. We obtained these measurements using simulated waste. Testing used a nitrogen flow rate of 15 cc/min to the vessel with 6 scfh supplied to the shroud.

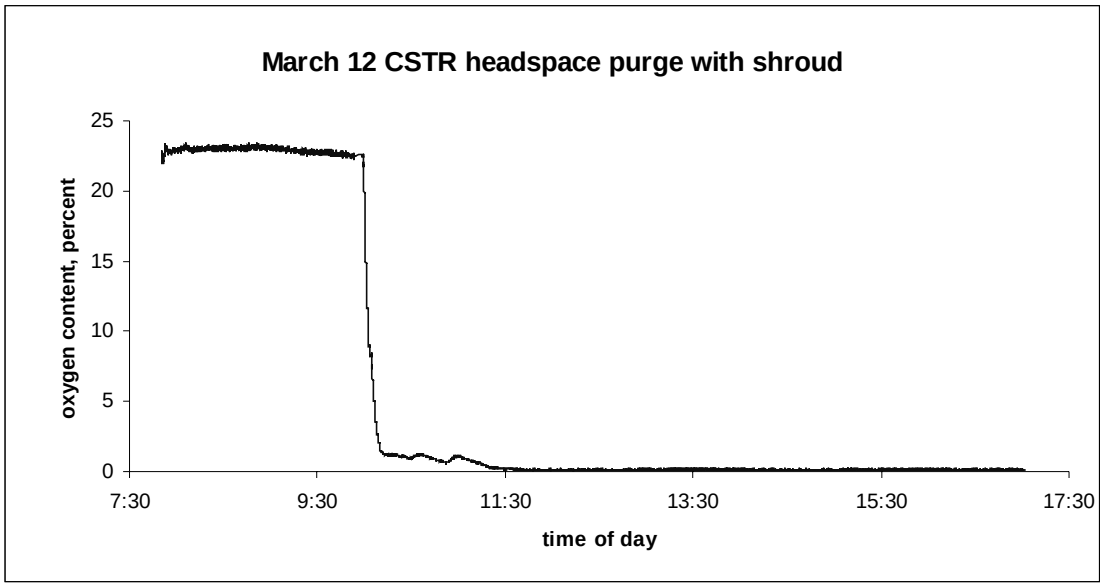

Figure 17. CSTR 24 hour test oxygen levels. The system rapidly reached <1 vol % oxygen after the purge lines were activated.

Note the initial oxygen depletion as the test starts (shortly after 9:30). The data before that time demonstrates the stability of the probe in this application. Once personnel started the purges at 10:00 a.m., the headspace of the vessel rapidly depleted to less than 1 vol % oxygen. The rise in oxygen concentration at approximately 6:00 p.m. corresponds to depletion of nitrogen in the supply tank, necessitating replacement with a fully charged tank. The data indicates the design can achieve anoxic conditions through the use of a two-tiered nitrogen purge system using a total of 21 SCFH per CSTR.

3.4 Control System Description and Operation

The Control System for the CSTR System consists of a Modicon Quantum PLC controller model 113-02, associated Quantum I/O modules, and an industrial hardened workstation. The PLC programming utilizes the Site Licensed Taylor ProWORX Plus, version 1.55 software. The PLC code is standard 984LL ladder block diagram with the enhanced Quantum instruction set. The 28 PLC networks used for this test consists of latch logic for the motor run signals, scaling, and six single loop PID controllers with associated logic for setpoint tracking and bumpless transfer. The PLC logic is commanded through the HMI using the Modbus Plus communications protocol, an SA85 adapter, and associated cabling. The HMI is an industrial hardened workstation running Microsoft Windows NT™ Workstation version 4.0 and the Intellution Fix32™ version 7.0 HMI package. The HMI uses "poke points" to initiate motor START / STOP commands, collects and displays process data, provides alarms, and allows the operator to change setpoints for various process parameters. The HMI also collects serial data via the workstations two RS232 Communication ports using the Taltech WinWedge Pro 32 version 3.0c software. Serial data consists of two chillers. Chiller communications are bi-directional, utilizing closed loop setpoint control. If chiller communications are lost, the HMI places the chiller loop in manual mode, preventing integral windup in the PLC, and sounds an alarm. The HMIs Graphical User Interface (GUI) consists of 13 operator displays showing a system overview (Figure 18), alarm messages, and process graphs in both real-time and historical

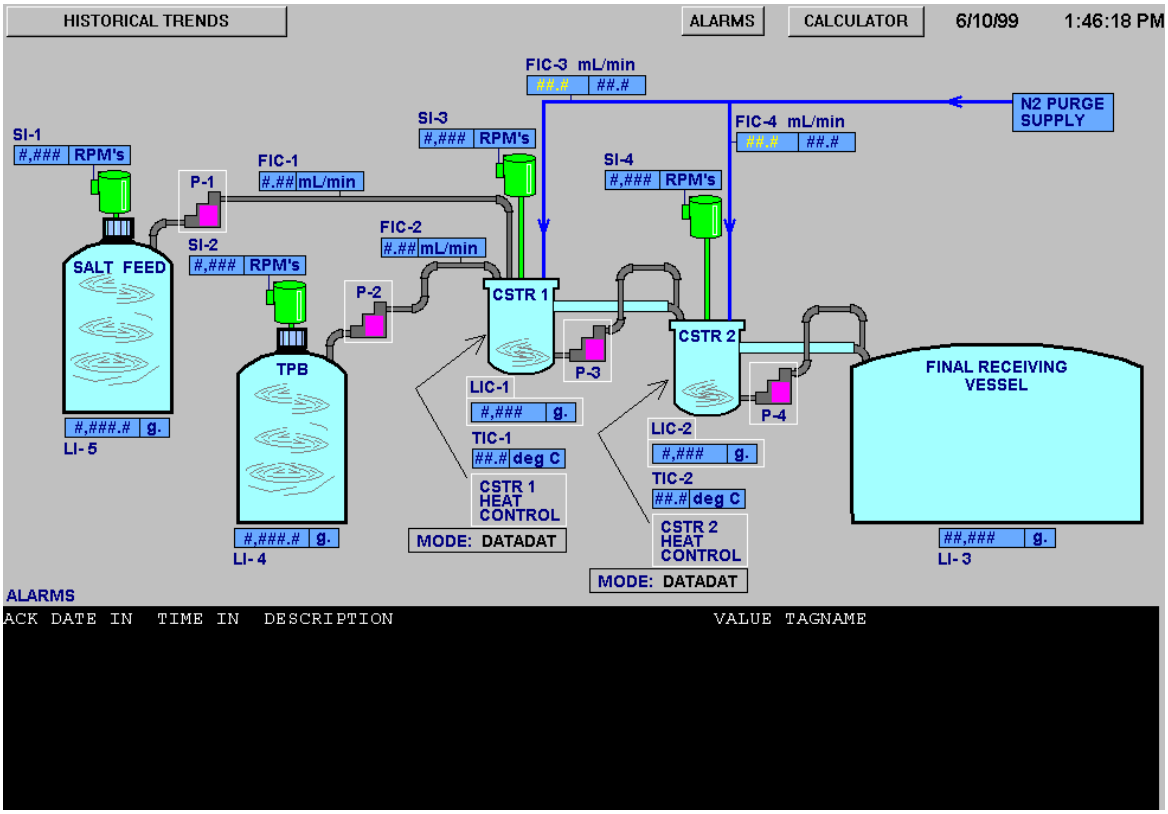

Figure 18. The Graphical User Interface for the equipment.

data (Figure 19). The HMI uses point-and-click functionality for commandable devices, setpoint changes, and moving between the process graphics. All HMIs meet the Human Factors criteria of the U.S. Nuclear Regulatory Commission report NUREG 0700, Rev.1, "Human System Interface Design Review Guidelines", the recognized standard at the Savannah River Site.

3.5 Experimental Approach – Simulated Waste

Before installation in the shielded cells, the experimental design included a complete set of calibration and performance tests using simulated waste to uncover any potential flaws in design or operation.

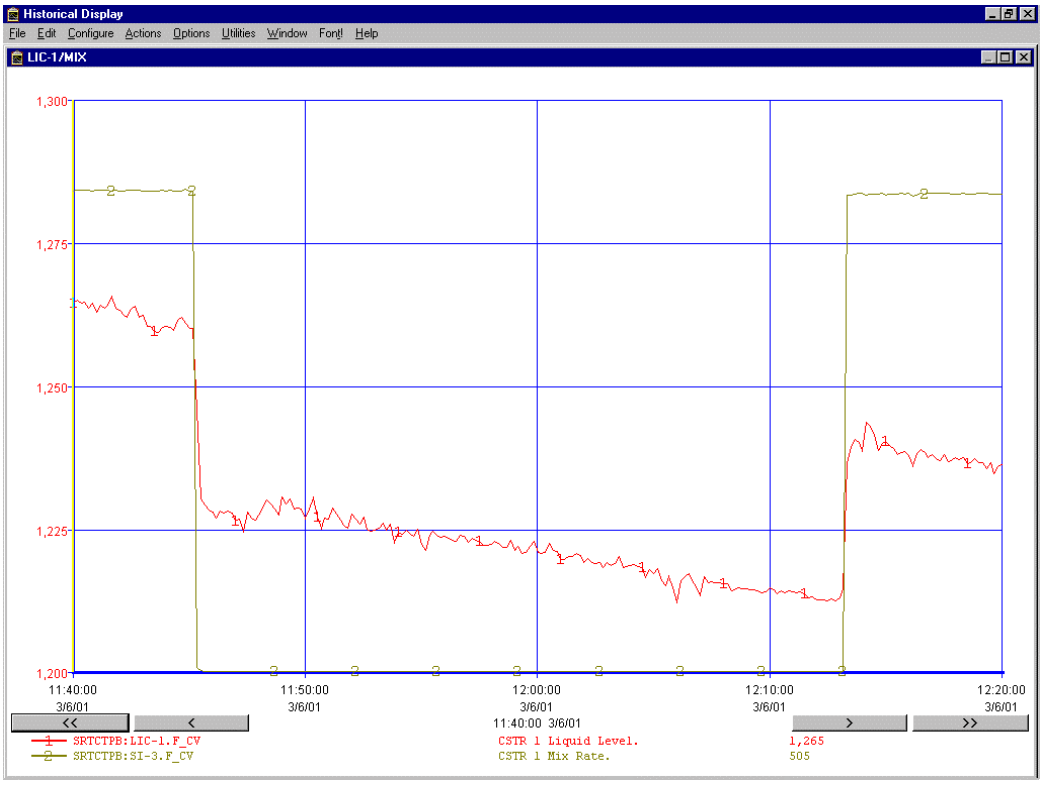

Figure 19. A Typical View of Some Historical Data Trends.

3.5.1 The Calibration Run

The calibrations checked the individual pieces of equipment for the potential of failure or operation outside of specifications. The process instrumentation consists of two thermocouples, load cells, flow meters, and positive displacement metering pumps as the final control elements. We verified the two thermocouples using NIST traceable M&TE equipment. The load cells calibration used standard masses and raw input counts collected at the PLC. A linear regression performed on the collected data using other software tools provided a best fit first order polynomial equation that we implemented in the PLC. We “barrel” tested the flow transmitters and final control elements using graduated glassware verified by lab personnel and the Techmation Protuner 32 software. Protuner 32 is a software package used for process analysis and system tuning. This version operates under Windows NT and can utilize the use of OPC client server software to communicate directly with the PLC State Ram, using the Modbus protocol that provides faster data collection, and the ability to analyze conditioned signals and setpoints not traditionally available at the I/O. Following calibration and verification of all instrumentation, prersonnel characterized the control loops by stepping each of the final control elements through its full range of operation looking for hysteresis and system nonlinearity. These tests yielded a series of tuning steps and tuning parameters.

Testing identified the following flaws that personnel corrected:

- The original design delivered MST in the NaTPB/dilution water feed, and the MST settled in the pump feed lines due to the low feed flows. This discovery led to the construction of a separate MST addition funnel and line, and removal of MST from the NaTPB/dilution water feed. For the final design, personnel added MST in small volumes, every two hours, to approximate the continuous addition.

- The nitrogen purge into the vessels proved insufficient to make the reactive system anoxic. Personnel constructed a shroud above each reactor to address this concern (see Section 3.3, above).

- Two of the stirrer shafts required replacement to prevent excessive vibration of the feed bottles.

- Personnel moved several of the cable connectors to positions more accessible for the remote operations.

3.5.2 Simulated Waste Tests

The simulated waste test used conditions as close as possible those that expected in the high-level waste test. To this end, personnel assembled the apparatus in the Mock Up Cells (Figure 20). The Mock Up Cells have nearly the same dimension and use remote operating arms similar

Figure 20. Mock Up Cells Area

to those in the shielded cells. This approach allowed the operators to practice the required evolutions and practice assembly of the equipment racks. The first test with simulated waste lasted four days. The test proceeded according to a written procedure.[6] Two researchers and two cells operators attended at all times. During this time, personnel did not observe any foaming other than minor frothing in the sampling process. However, researchers did note that the data indicated multiple instances of slurry accumulation in the vessel as demonstrated by changes in liquid level, followed by a rapid clearing of the overflow passages (Figure 21). Personnel collected samples for analyses every four hours with MST added every two hours.

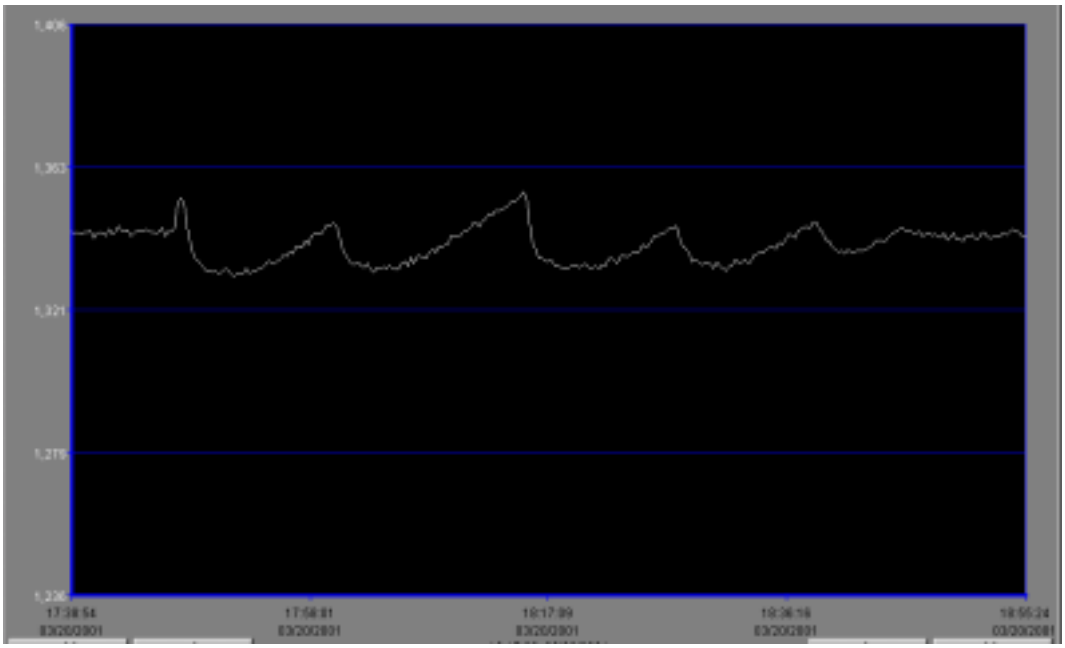

Figure 21. Data Trend Showing Slurry Hold Up and Clearing.

After ~2.5 system turnovers, personnel verified that decontamination (via potassium tracking) occurred, and so they increased the temperature in the experiment to 45 °C. The experiment continued another 2 system turnovers at that temperature. Overall, the test proceeded smoothly, with no outages or troubles. Section 4.1 discussed the analytical data and results from the experiment.

After the test, the project management reached a decision that only a selected batch of the antifoam met program needs. Unfortunately, the simulated waste experiment used a different, “non-baseline” B-52 (IITB-52-10-5-2000 LOT #CKWAN). Hence, we needed to conduct an additional demonstration using the baseline version of the antifoam (IITB-52-9-14-2000, lot # ANAEPG) and simulated waste. The second test lasted 1.5 system turnovers and included only an assessment of system hydraulics. The testing completed without any observed hydraulic problems.

In conclusion, the simulant runs proved that the apparatus could function successfully under the same conditions as anticipated in the shielded cells. Although the apparatus functioned well, experiences during the tests prompted minor modifications:

- We enlarged the MST funnel for easier pouring
- Personnel added electrical quick connects between the main and receipt racks for the chillers
- We replaced the syringe pump for a less radiation damage susceptible unit (KD Scientific Model 101)
- We redesigned the mounting for the CSTRs to prevent movement of the CSTRs
- We adjusted the level, calibrated, and rebalanced all four of the 6 kg load cells
- All the feed lines were marked with color coded tape for easier remote assembly
- Nitrogen lines for the shrouds were added along with quick connect lines
- An additional lifting bracket was added to the feed rack
- The 19 and 55 plug heads were visually marked for easier remote operations

3.6 Experimental Approach – High Level Waste

After assembly of the equipment in the shielded cells, personnel noted difficulties in establishing control for the various pumps and chillers. Inspection identified damaged electrical pins on one of the connectors. Fortunately, the damaged pins were repaired through the use of a clever tool designed on site (see Appendix 2), which caused us to take only a 24-hour delay in the schedule.

The experiment with high-level waste lasted eleven days, and proceeded according to a written procedure.[6] Testing included a four-day experiment similar to that using simulated waste followed by a one week observation period at the elevated temperature. During this time, personnel did not observe any foaming but did note that as time progressed (but before the temperature was increased to 45 °C) the samples became slightly more "frothy". After increasing the temperature to 45 °C, the samples appeared much thinner in consistency, likely due to decreasing viscosity as temperature increases. Personnel collected samples for analyses every four hours with MST added every two hours. After ~2.5 system turnovers after achieving DF (61 hours) of operations, personnel increased the temperature in the vessels to 45 °C. After ~0.5 system turnovers (10 hours) at 45 °C, the overflow line from CSTR#1 to CSTR#2 clogged and no longer allowed slurry transfer. After waiting for 55 minutes, personnel judged that the line would not clear and decided to activate the backup pump to control liquid level. This pump ran flawlessly for the remainder of the experiment and provided excellent level control. The experiment continued another ~1.5 system turnovers (22 hours) at that temperature, at which time the experiment ended. After 2 system turnovers after achieving DF (32 hours) of testing at 45 °C, the researchers halted the feed flows and maintained the slurries in the reactors at 45 °C, with nitrogen flow and agitation, for an additional seven days. Personnel collected samples once per day during this time. During this time, we kept the volume in CSTR#2 relatively constant volume by drawing slurry from CSTR#1. Testing proceeded without any notable events. Chiller

#2 failed after ~4.5 system turnovers (5 days and 19 hours) in the seven day period, probably due to radiation damage. Chiller #1 failed within 24 hours after the end of the test.
After this week, personnel stopped the test but maintained stirring in CSTR#2, to prevent excessive settling of the slurry.

4.0 RESULTS AND DISCUSSION

4.1 Simulant Test Results

The test with simulated waste used a solution prepared to mimic the high-level waste solution. Table 2 shows the composition. The solution had a final sodium concentration of 10.3 M and a

Table 2. Composition of the Simulated Waste Solution

Contents	Concentration (M)
Na^+	10.3
K^+	0.084
Cs^+	0.00084
OH^-	6.2
NO_3^-	1.91
NO_3^-	1.55
$Al(OH)_4^-$	0.27
CO_3^{2-}	0.18
SO_4^{2-}	0.013
PO_4^{3-}	0.01

measured density of 1.39 g/mL. Personnel controlled the flows of the simulated waste to 0.99 mL/min while adding the NaTPB/dilution water (i.e., 0.55 M in NaTPB and 0.1 M in NaOH) at 1.06 mL/min. Personnel added MST every two hours to maintain an average MST concentration of 0.4 g/L in the first vessel assuming ideal mixing. Operators collected slurry samples using a standard protocol. First, they purged the sample line for ~15 minutes before collecting ~30 mL of slurry in a small plastic polyethylene bottle. Operators filtered the samples using 100-mL (0.45μ porosity) filter cups, reserving the liquid for analysis and discarding the solids. Researchers analyzed the resulting 21 samples for sodium, potassium, strontium, total soluble boron, and phenylborates.

4.1.1 Strontium Results

Removal of strontium was an important objective for the test using simulant waste. The ADS personnel analyzed samples for strontium content via ICP-MS. While we added no strontium to the simulant waste recipe, it was felt that historical precedents showed enough tramp strontium

would be present to get a good DF measurement. The results the analyses showed strontium levels were below detection limits (250 μg/L) in every case but the very first sample. ADS personnel re-analyzed samples, using using ICP-ES. From the new analyses, the results showed all samples to have less than detectable (90μg/L) strontium levels. Due to this lower than expected strontium levels, the researchers were unable to determine a strontium DF value for the MST.

4.1.2 Sodium Results

The ADS personnel analyzed samples for sodium content via AA. The starting sodium value of the salt simulant was 10.3 M by design. Once mixed with the NaTPB/dilution water, the final

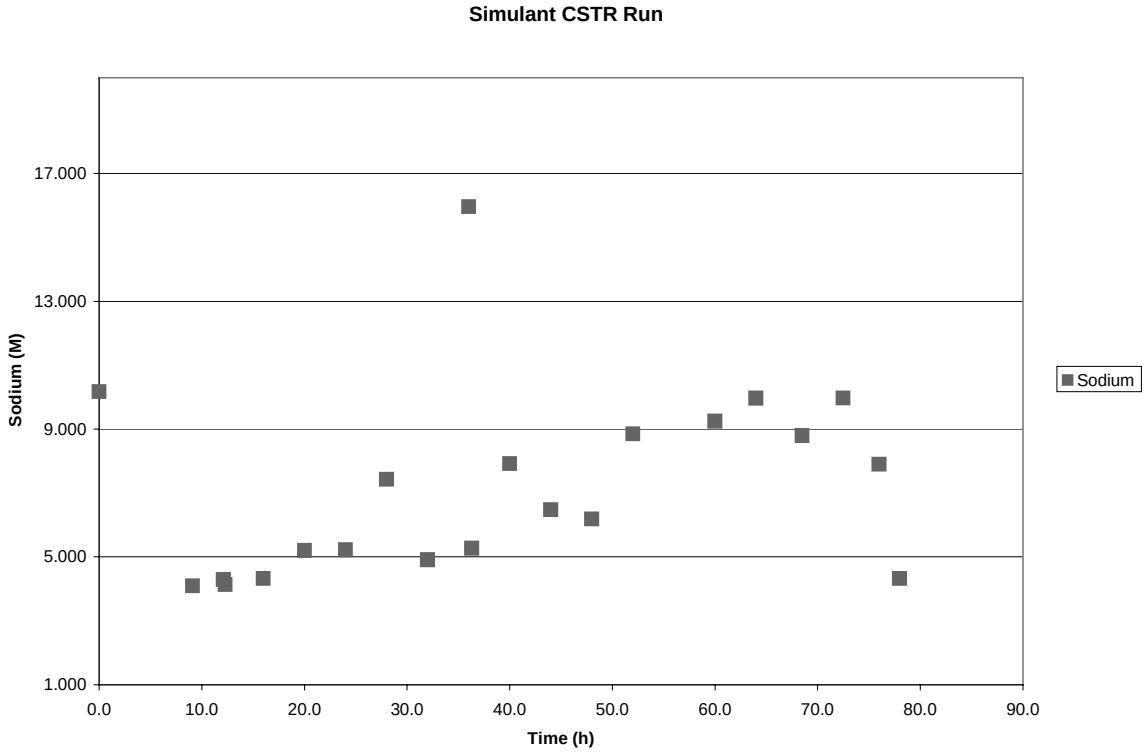

Figure 22. Sodium Concentration in Samples From Test Using Simulated Waste.

sodium concentration was targeted to be 4.7 M. Over the period of the simulant run, the sodium results (Figure 22) showed a large variance. Due to this scatter, the samples were re-analyzed, The new analysis provided results that were typically neither precise nor accurate. The researchers feel that instrumental problems are responsible for the large variances.

4.1.3 Potassium Results

ADS personnel analyzed samples for potassium content via AA. The starting potassium value of the salt simulant was formulated to be 0.084 M. As cold cesium is difficult to monitor at low

concentrations, potassium was used as a "DF surrogate" for cesium. Data collected throughout the experiment (Figure 23) shows that the potassium concentration drops quickly (reaching detection limits by ~12 hours) and remains at a level beneath the analytical detection limits of

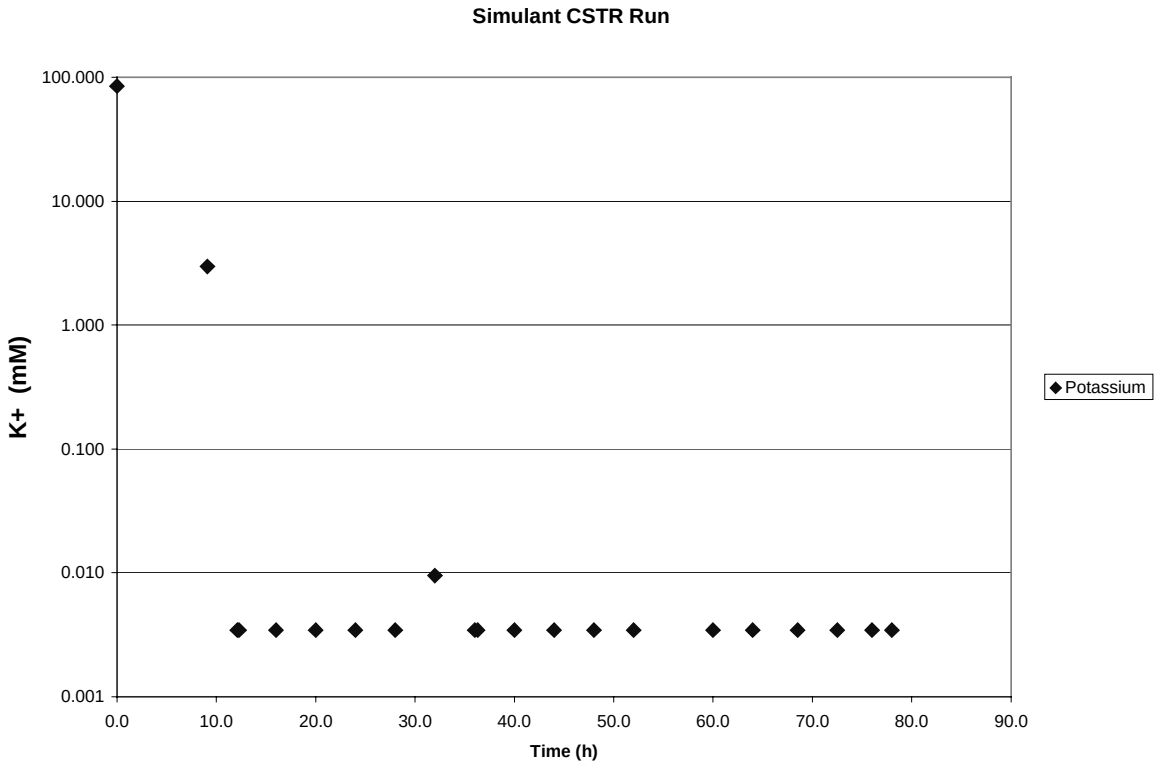

Figure 23. Potassium Concentration in Simulant Run Samples.

0.135 mg/L (3.46E-03 mM), except for a single result which we believe to be contaminated sample or an analytical flier. If we assume that the potassium concentration is just at the detection limit, then the potassium reaches a DF[†] of 11,121 after about ~12 hours and remains there, even at higher temperature. As cesium has a lower solubility limit than potassium, this produced an even higher DF value for cesium (Ksp [CsTPB] = ~1.2×10^{-11} M^2 at 25 ºC, Ksp [KTPB] = ~3.8×10^{-8} M^2 at 25 ºC).[14]
The experiment clearly met the objective of decontaminating the waste and maintaining performance for the duration of testing.

4.1.4 HLPC Phenylborate results
The ADS personnel analyzed samples for TPB and its decomposition products content via HPLC. The NaTPB/dilution water contained a 60% stoichiometric excess compared to the

[†] The DF value takes into account the initial dilution of the 10.3 M sodium salt feed to 4.7 M sodium.

combined cesium and potassium concentrations. The data (Table 3) indicates that there are no detectable amounts of 3, 2, 1PB, or phenol. This, in turn, shows that TPB decomposition

Table 3. Phenylborate Data from HPLC Analyses of Samples During Simulant Run.

Sample ID	Time (h)	NaTPB (mg/L)	3PB (mg/L)	2PB (mg/L)	1PB (mg/L)	Phenol (mg/L)
C1-Feed0-SIMSTTP-2	0.0	< 10	< 10	< 10	< 10	< 10
1-8-SIMSTTP-2	9.1	< 10	< 10	< 10	< 10	< 10
2-12-SIMSTTP-2	12.1	264	< 10	< 10	< 10	< 10
C2-12-SIMSTTP-2	12.3	281	< 10	< 10	< 10	< 10
3-16-SIMSTTP-2	16.0	296	< 10	< 10	< 10	< 10
4-20-SIMSTTP-2	20.0	252	< 10	< 10	< 10	< 10
5-24-SIMSTTP-2	24.0	230	< 10	< 10	< 10	< 10
6-28-SIMSTTP-2	28.0	194	< 10	< 10	< 10	< 10
7-32-SIMSTTP-2	32.0	156	< 10	< 10	< 10	< 10
8-36-SIMSTTP-2	36.0	157	< 10	< 10	< 10	< 10
C3-36-SIMSTTP-2	36.3	105	< 10	< 10	< 10	< 10
9-40-SIMSTTP-2	40.0	152	< 10	< 10	< 10	< 10
10-44-SIMSTTP-2	44.0	144	< 10	< 10	< 10	< 10
11-48-SIMSTTP-2	48.0	153	< 10	< 10	< 10	< 10
12-54-SIMSTTP-2	52.0	139	< 10	< 10	< 10	< 10
13-66-SIMSTTP-2	60.0	143	< 10	< 10	< 10	< 10
14-70-SIMSTTP-2	64.0	142	< 10	< 10	< 10	< 10
15-74-SIMSTTP-2	68.5	119	< 10	< 10	< 10	< 10
16-78-SIMSTTP-2	72.5	129	< 10	< 10	< 10	< 10
17-82-SIMSTTP-2	76.0	128	< 10	< 10	< 10	< 10

is extremely slow or non-existent. We did not explicitly add a catalyst to promote decomposition. The slowly decreasing amount of TPB (Figure 24) in solution is not due to decomposition, but is likely due to changing (i.e., minor fluctuations) salt content over the time of the test. As the salt content increases, the solubility of the TPB decreases. While we cannot derive precise trends from the sodium data, an overall increase in sodium concentration is noted.

4.1.5 Total Soluble Boron

The ADS personnel analyzed samples for total soluble boron using a combination of microwave dissolution and ICP-ES. This method uses a filtration to remove undissolved solids, followed by a microwave dissolution of the filtrate. Finally, ICP-ES is used to measure the concentration of boron in the sample. If there is TPB decomposition occurring, the dissolution of NaTPB to

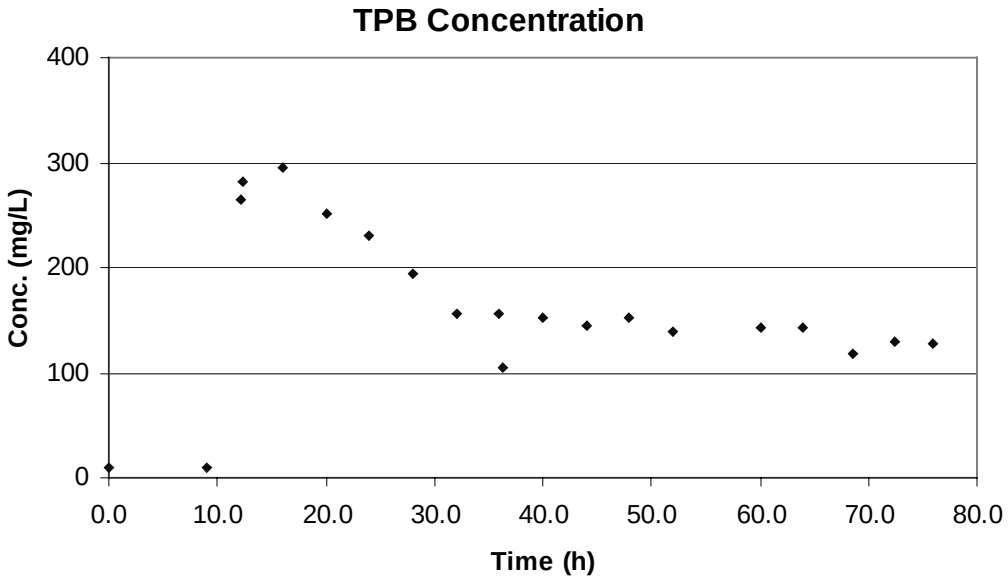

Figure 24. TPB Concentration Over Time.

replace decomposing NaTPB will increase the total soluble boron. However, the data (Figure 25) shows that after the initial soluble boron increase at the start, the total soluble boron content

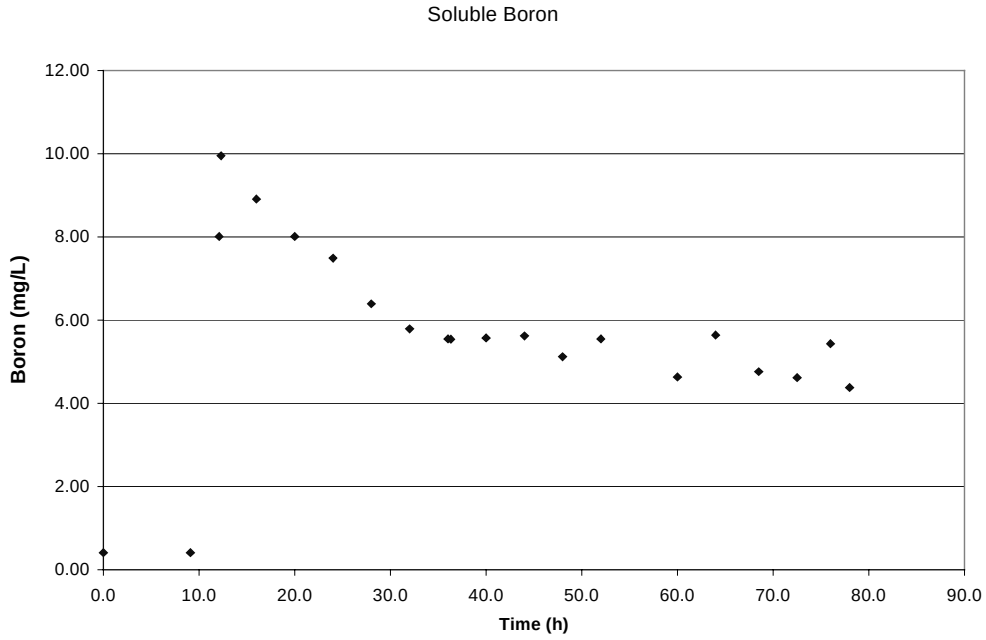

Figure 25. Measurements of the Total Soluble Boron.

decreases over time. This matches the observation of the decreasing NaTPB values shown in section 4.1.4. As there is less TPB in solution over time, there is less boron in solution.

4.2 Real Waste Test Results

A standard procedure dictated the sampling schedule and method.[6] Personnel controlled the flows of the simulated waste to 0.94 mL/min while adding the NaTPB/dilution water (i.e., 0.122 M in NaTPB and 0.1 M in NaOH) at 1.12 mL/min. Personnel added MST every two hours to maintain an average MST concentration of 0.4 g/L in the first vessel assuming ideal mixing. Operators collected slurry samples using a standard protocol. First, they purged the sample line for ~15 minutes before collecting. Then, ~30 mL of slurry was collected into a 100 mL (0.45µ porosity) filter cup. The solids were filtered off, and the filtrate collected for analysis.
Over the course of the four day real waste run, personnel collected 30 slurry samples which were filtered, and analyzed for: gamma activity (cesium), sodium, potassium, strontium, plutonium, actinides plus fission products, total soluble boron, and phenylborates. This gave a total of 240 different analyses.

4.2.1 Cesium Results

One of the primary objectives of this experiment is to demonstrate sufficient DF for cesium. ADS personnel analyzed for cesium content via gamma scan, which counts the gamma activity of the barium-137(m) daughter. The cesium activity is 3670 uCi/mL (3060000 nCi/g - assumes

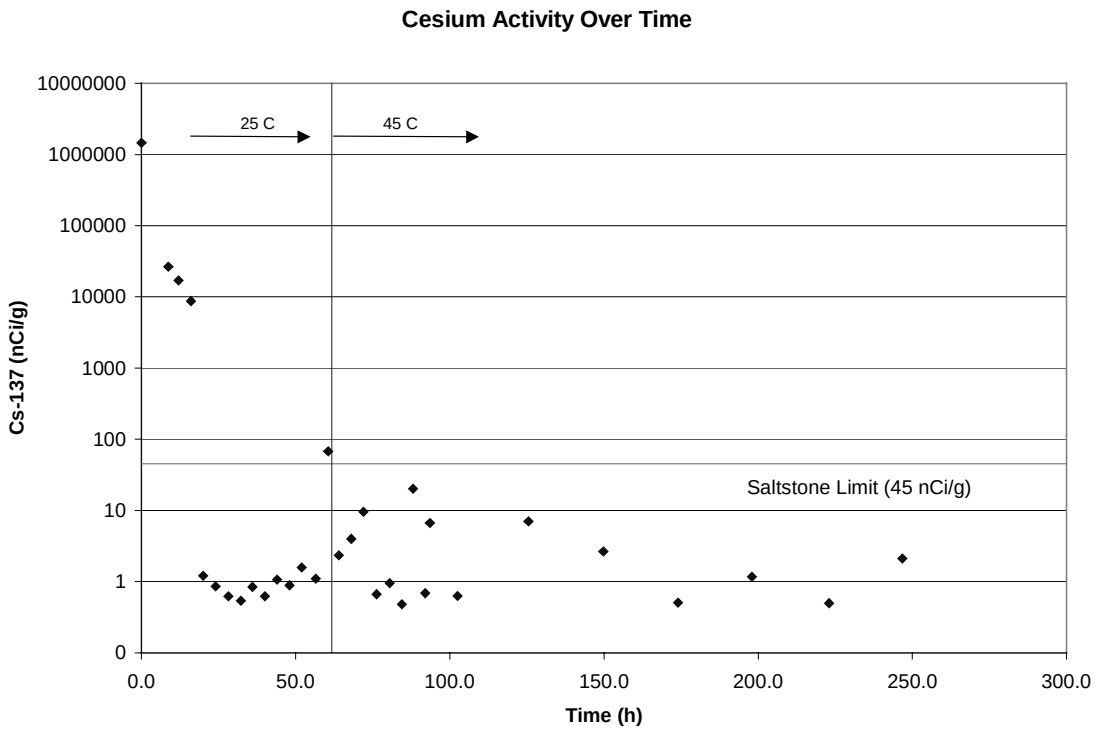

Figure 26. Cesium-137 Activity Over Time.

density =1.48) in the salt waste solution (before any dilution). As the experiment progresses, more and more of the cesium precipitates out of solution as cesium tetraphenylborate, CsTPB. Once steady-state is reached, the cesium content in solution remains constant except for flow variances. The filtrate, then, contains less and less cesium, until remaining constant at steady state. The results of the data (Figure 26) show that as time progresses, the cesium activity decreased dramatically. By about the time of the fourth sample (~16-20 hours, ~1 system turnover), the cesium activity dropped below the limits imposed by the Saltstone facility; 45 nCi/g. Accordingly, after ~1 system turnover (20 hours), the process has achieved a DF value of 1.15 million. In reality, the all but two post-steady-state DF values this experiment generated were much higher; some reaching as high as ~3 million (Table 4). The increase in temperature to 45 °C seemed to slightly decrease the average DF, as expected due to solubility shifts.

Table 4. Cesium Activity and DF Achieved in Each Sample.

Sample ID	Time (h)	Avg. Cs-137 (nCi/g)	DF
0-0-STTP-2	0.0	1158486	0.456
1-8-STTP-2	8.8	26472	53
2-12-STTP-2	12.0	17045	82
3-16-STTP-2	16.0	8687	161
4-20-STTP-2	20.0	1.2	1154182
5-24-STTP-2	24.0	0.9	1630117
6-28-STTP-2	28.3	0.6	2255556
7-32-STTP-2	32.3	0.5	2599113
8-36-STTP-2	36.0	0.8	1655743
9-40-STTP-2	40.0	0.6	2253174
10-44-STTP-2	44.0	1.1	1309095
11-48-STTP-2	48.0	0.9	1567550
12-52-STTP-2	52.0	1.6	884239
13-56-STTP-2	56.5	1.1	1274815
14-60-STTP-2	60.5	67.4	20700
Temperature Increased to 45 °C			
15-64-STTP-2	64.0	2.3	620675
16-68-STTP-2	68.0	4.0	362522
17-72-STTP-2	72.0	9.6	151195
18-76-STTP-2	76.3	0.7	2177123
19-80-STTP-2	80.5	0.9	1523173
20-84-STTP-2	84.5	0.5	3021688
21-88-STTP-2	88.0	20.0	72097
22-92-STTP-2	92.0	0.7	2107210
A-93.5-STTP-2	93.5	6.6	217733
23-122-STTP-2	102.5	0.6	2309495

24-146-STTP-2	125.5	7.0	198617
25-170-STTP-2	149.8	2.6	527685
26-194-STTP-2	174.0	0.5	2759208
27-218-STTP-2	198.0	1.2	1198454
28-242-STTP-2	223.0	0.5	2812050
29-266-STTP-2	246.8	2.1	661856

The one data point that does not meet DF and saltstone requirements (after reaching steady-state) is from sample 14-60-STTP-2. A duplicate analysis of this sample (from the same bottle) showed approximately the same results, so analytical error has been ruled out. A potassium analysis of the same sample also showed an anomalous spike. Considering the nature of the data points surrounding it in time, the researchers feel that this sample suffered from contamination from its time in the high activity cells, and not a failure of the process. Due to the consistent and high DF values achieved, the requirement for cesium removal was demonstrated successfully.

4.2.2 Strontium Results

Another important objective for this experiment was the removal of strontium and other actinides. The ADS personnel analyzed the samples for strontium content via beta scintillation counting. Strontium exists in the real salt waste solution at 5,550,000 dpm/mL (869 nCi/g) (before accounting for the dilution the salt feed undergoes in the CSTR). Examination of the data (Figure 27) shows that after steady state, the regular MST addition causes the successful

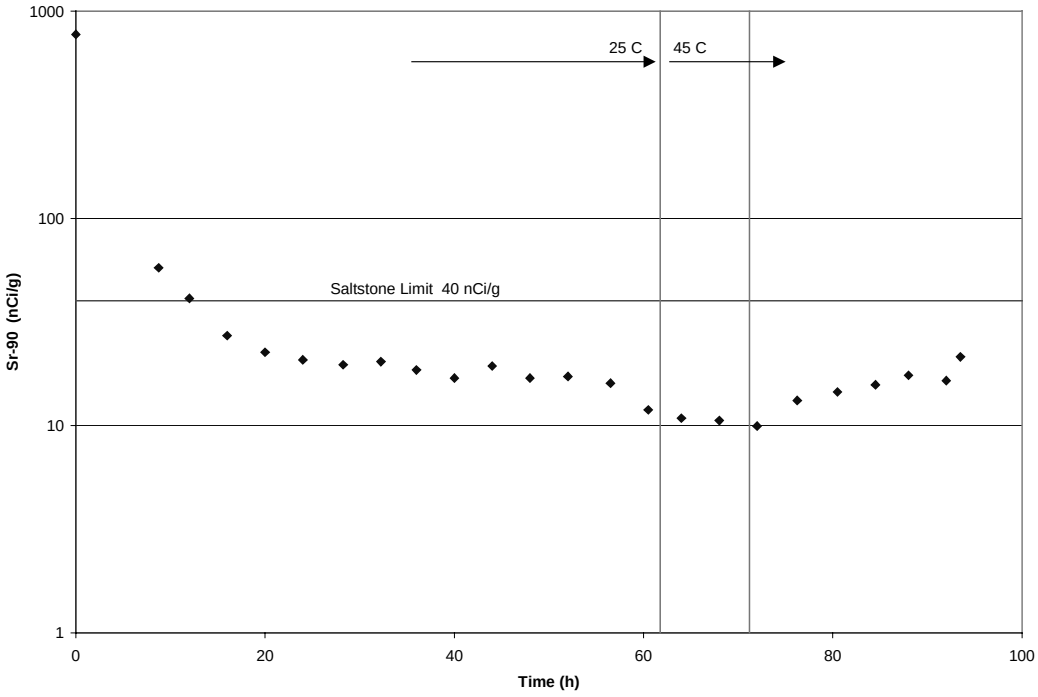

Figure 27. Strontium Activity Over Time.

decontamination of strontium. By the time of the fourth sample (~16 hours), the strontium activity dropped to below the Saltstone limits, which requires a DF of ~22, or 40 nCi/g. The process achieved DF at every sample, and went as high as 77. The DF values are approximately comparable to previous tests involving MST.[15] The change in temperature to 45 °C did not seem to affect the strontium DF. See Appendix 3 for tabular data.
Even though the MST was not added in a strictly continuous nature, it effectively and quickly removed enough of the strontium to meet Saltstone requirements and to declare success.

4.2.3 Removal of Plutonium and Uranium

Besides strontium, this experiment was designed to remove actinides such a plutonium and uranium. ADS personnel analyzed for plutonium content via PuTTA and for uranium content via RADICP-MS. The real salt waste solution contained plutonium at 63900 dpm/mL for ^{238}Pu and 1860 dpm/mL for $^{239/240}$Pu (after accounting for the dilution the salt feed undergoes in the reaction). The real salt waste solution contained uranium at 68.7 dpm/mL for ^{233}U, 0.815 dpm/mL for ^{235}U, and 2.65 dpm/mL for ^{238}U (after accounting for the dilution the salt feed undergoes in the reaction).
An analysis of the Plutonium-238 data (Figure 28) shows that the plutonium concentration dropped rapidly, reaching an average concentration of 1.33E-05 mg/L. This in turn gives an average DF of 126.[#] The plutonium-239/240 data is more difficult to analyze due to the inability

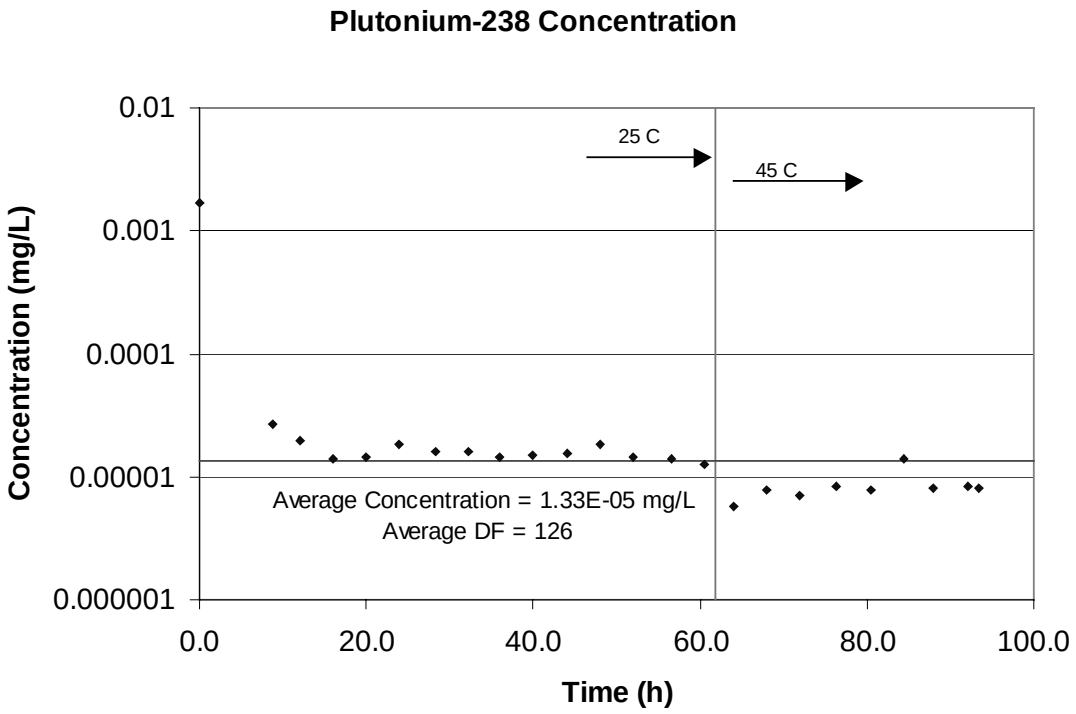

Figure 28. Total Plutonium Concentration Over Time.

[#] This is calculated as a simple average and does not use the time=0 data point (before steady state).

to deconvolute the two isotopes; but following the same rationale, achieved an average DF of 83.3. An analysis of the Uranium data (Figure 29) shows that the total uranium concentration dropped rapidly, reaching an average concentration of 1.63 mg/L. This in turn gives an average DF of 2.36.[$] This DF value is approximately comparable to previous tests involving MST.[15] See Appendix 3 for tabular data.

The driving force for the removal of actinides is the Saltstone Facility Waste Acceptance Criteria of a total alpha dose of 20 nCi/g or less.[9] When the activities of the plutonium and uranium are totaled for each data point, the result can be plotted against the Saltstone WAC (Figure 30). The data shows that against a starting value of 24.7 nCi/g for the real salt waste, the activity drops rapidily to an average of 0.214 nCi/g. This gives an average DF of 155, compared to a required DF of 1.24. The changes in temperature from 25 °C to 45 °C seemed to have no effect against the DF. Even though the MST was not added in a strictly continuous nature, it effectively and quickly removed enough of the strontium to meet Saltstone requirements and to declare success.

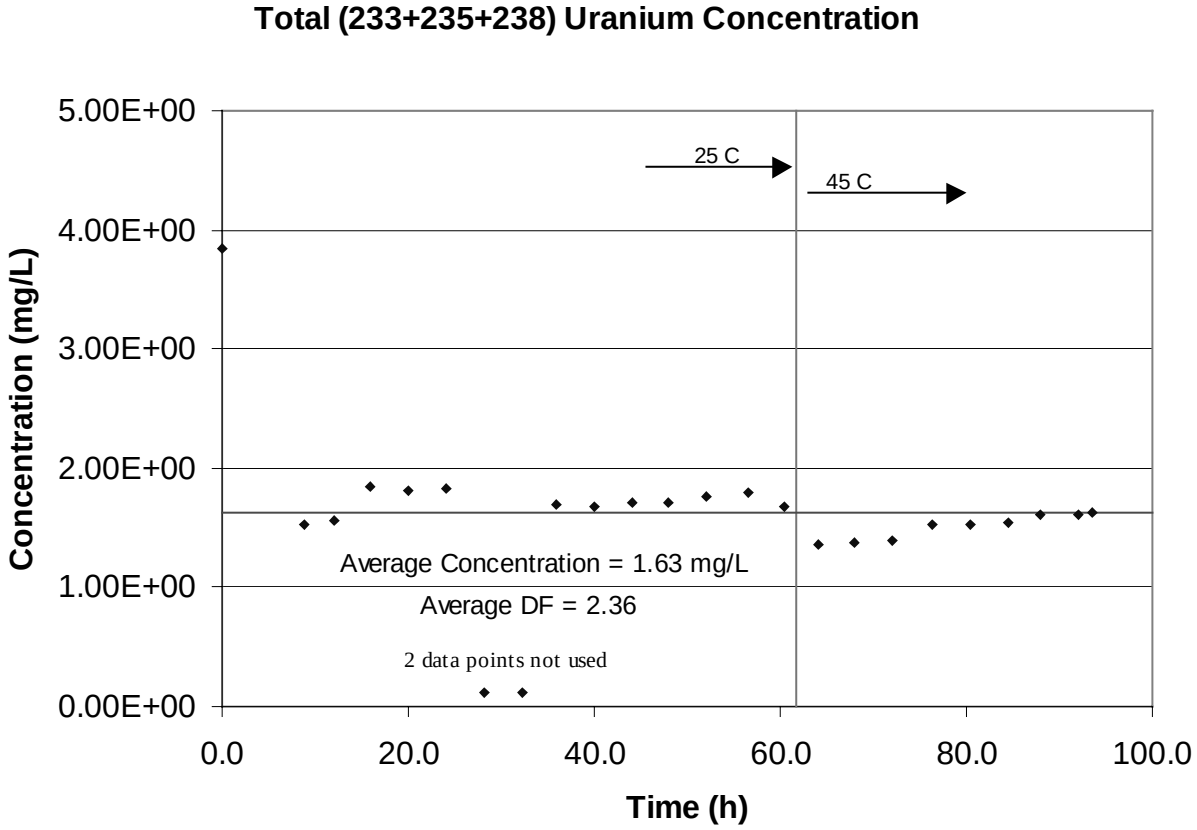

Figure 29. Total Uranium Concentration Over Time.

[$] This is calculated as a simple average and does not use the time=0 data point (before steady state).

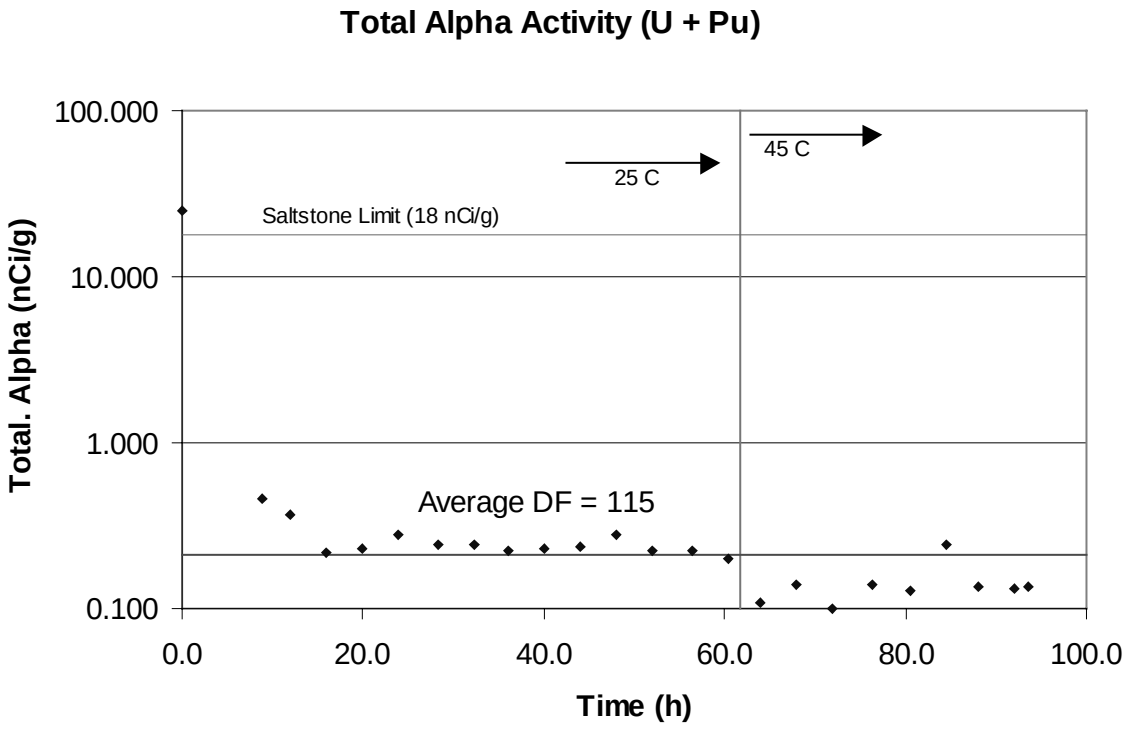

Figure 30. Total Alpha Activity Over Time.

4.2.5 Sodium Results

The ADS personnel analyzed the samples for sodium content via AA. The starting sodium value of the waste salt solution was 10.25 M by measurement. Once mixed with the NaTPB/dilution water, the final sodium concentration was designed to be 4.7 M. The data shows (Figure 31) that during the test the sodium level quickly reached the 4.7 M target area and maintained that approximate value throughout the test. While the target was 4.7 M, the average of the steady-state concentration was slightly low; 4.46 M. The differences can be attributed to slight variances in flow rates of the feed solutions. The change to 45 °C seemed to cause no difference in the sodium concentration. See Appendix 3 for tabular data.

4.2.6 Potassium Results

The ADS personnel analyzed the samples for potassium content via AA. The starting potassium value of the salt waste solution was 0.082 M by measurement. Data collected throughout the experiment (Figure 32) show that the potassium concentration drops quickly (reaching detection limits by ~20 hours). The concentration remains at a level beneath analytical detection limits of 0.135 mg/L (3.46E-03 mM), except for a single result, which we believe to be contaminated sample. Note that this "flier" was from the same filtrate sample (14-60-STTP-0) that gave the

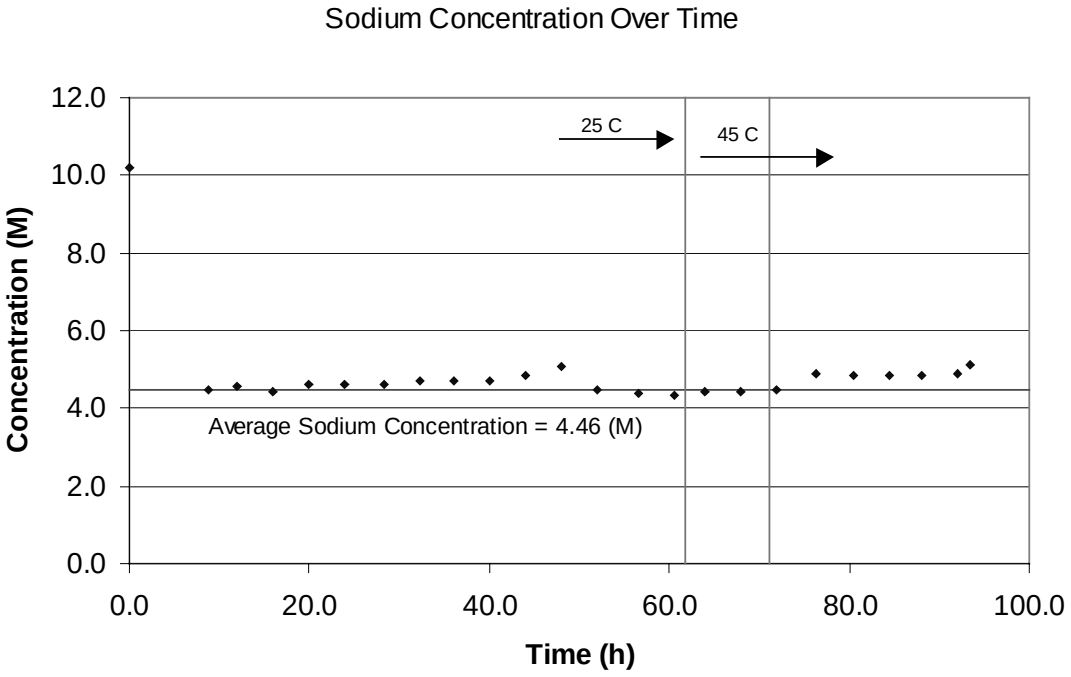

Figure 31. Sodium Concentration Over Time.

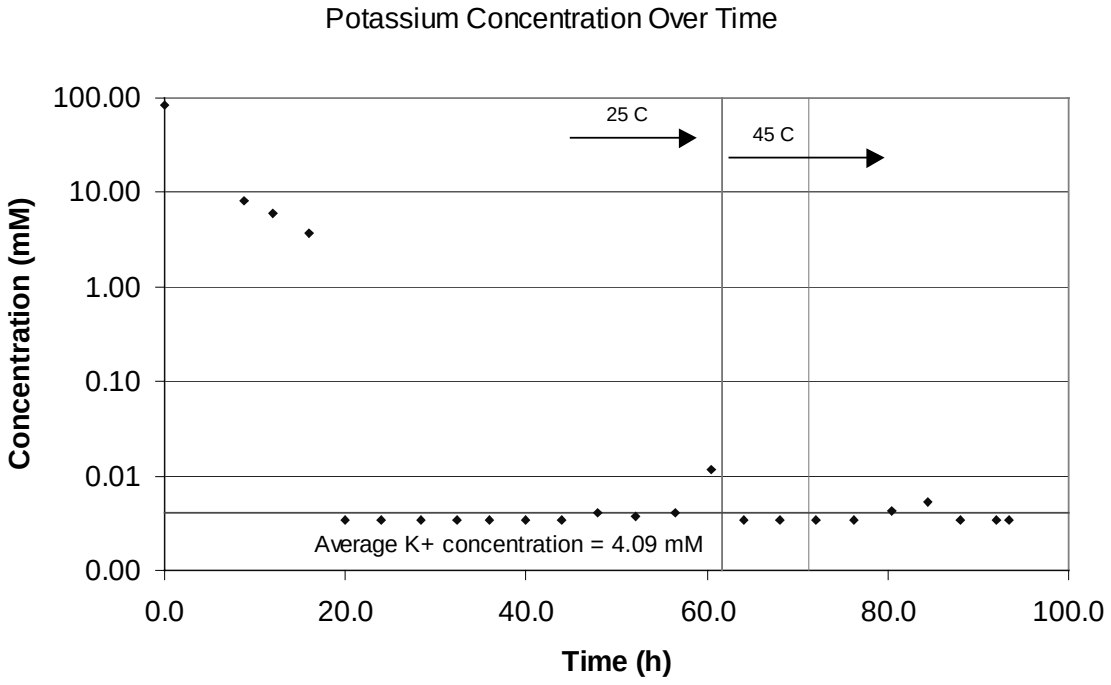

Figure 32. Potassium Concentration Over Time

"flier" for cesium results, thus reinforcing the researchers theory that this sample suffered from contamination. See Appendix 3 for tabular data.

4.2.7 HLPC Phenylborate results

The ADS personnel analyzed samples for TPB and its decomposition products via HPLC. The NaTPB/dilution water contained a 60% stoichiometric excess target compared to the combined cesium and potassium concentrations. The data (Table 5) indicates that throughout the experiment there were no detectable amounts of 3, 2, 1PB, or phenol. The varying amount of TPB in solution is not due to decomposition, but due to changing solubility limits in the high salt solution. The slight decline in NaTPB values matches the slight increase in sodium concentration over the course of the experiment.

Table 5. Phenylborate Concentrations Over Time During Real Waste Run.

Sample ID	Time (h)	NaTPB (mg/L)	3PB (mg/L)	2PB (mg/L)	1PB (mg/L)	Phenol (mg/L)
0-0-STTP-6	0.0					
1-8-STTP-6	8.8	< 1000	< 1000	< 1000	< 1000	< 1000
2-12-STTP-6	12.0	< 1000	< 1000	< 1000	< 1000	< 1000
3-16-STTP-6	16.0	< 10	< 10	< 10	< 10	< 10
4-20-STTP-6	20.0	78	< 10	< 10	< 10	< 10
5-24-STTP-6	24.0	73	< 10	< 10	< 10	< 10
6-28-STTP-6	28.3	65	< 10	< 10	< 10	< 10
7-32-STTP-6	32.3	53	< 10	< 10	< 10	< 10
8-36-STTP-6	36.0	61	< 10	< 10	< 10	< 10
9-40-STTP-6	40.0	75	< 10	< 10	< 10	< 10
10-44-STTP-6	44.0	58	< 10	< 10	< 10	< 10
11-48-STTP-6	48.0	46	< 10	< 10	< 10	< 10
12-52-STTP-6	52.0	63	< 10	< 10	< 10	< 10
13-56-STTP-6	56.5	48	< 10	< 10	< 10	< 10
14-60-STTP-6	60.5	31	< 10	< 10	< 10	< 10
15-64-STTP-6	64.0	65	< 10	< 10	< 10	< 10
16-68-STTP-6	68.0	68	< 10	< 10	< 10	< 10
17-72-STTP-6	72.0	72	< 10	< 10	< 10	< 10
18-76-STTP-6	76.3	67	< 10	< 10	< 10	< 10
19-80-STTP-6	80.5	64	< 10	< 10	< 10	< 10
20-84-STTP-6	84.5	51	< 10	< 10	< 10	< 10
21-88-STTP-6	88.0	67	< 10	< 10	< 10	< 10
22-92-STTP-6	92.0	65	< 10	< 10	< 10	< 10
A-93.5-STTP-6	93.5	70	< 10	< 10	< 10	< 10
23-122-STTP-6	102.5	50	< 10	< 10	< 10	< 10
24-146-STTP-6	125.5	29	< 10	< 10	< 10	< 10
25-170-STTP-6	149.8	22	< 10	< 10	< 10	< 10

4.2.8 Total Soluble Boron

The ADS personnel analyzed samples for total soluble boron using a combination of microwave dissolution and ICP-ES. This method uses a filtration to remove undissolved solids, followed by **a microwave dissolution of the filtrate. Finally, ICP-ES is used to measure the**

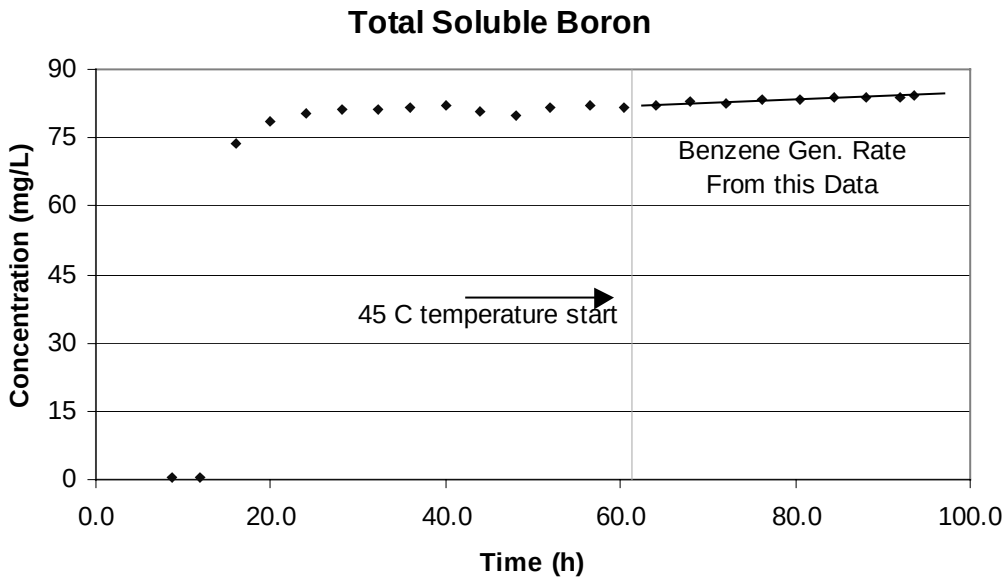

concentration of
Figure 33. Measurements of the Total Soluble Boron.

boron in the sample. If there is TPB decomposition occurring, the dissolution of NaTPB to replace decomposing NaTPB will increase the total soluble boron. However, the data (Figure 33) shows that after the initial soluble boron increase at the start (due to insoluble NaTPB going into solution), the total soluble boron content increases only slightly. See Appendix 3 for tabular data. The researchers regressed the total soluble boron data, during the time the experiment ran at 45 ºC. A statistically significant increase in boron yielded a theoretical benzene generation rate of 2.4 mg/(L•h), indicating a small amount of decomposition was occurring at 45 ºC.

4.2.9 RADICP-MS Results

The ADS personnel analyzed samples for soluble metal content via RADICP-MS. The results of the RADICP-MS were primarily used to determine the uranium concentration. The analysis also detected other metals; Zr, Tc-99, Mo, Ag, Pd, Rh, Ru, Cd, Sn, W, Ir, Re, Pt, Hg, Pb. Of these metals, the most catalytically active ones are Pd, Rh, Ru, Pt, and Hg. For Pd, Rh, and Ru, an examination of Figure 34 shows that each element achieves a reasonably constant concentration during the bulk of the experiment. This probably indicates a lack of involvement in any noticeable way in the decomposition of TPB.

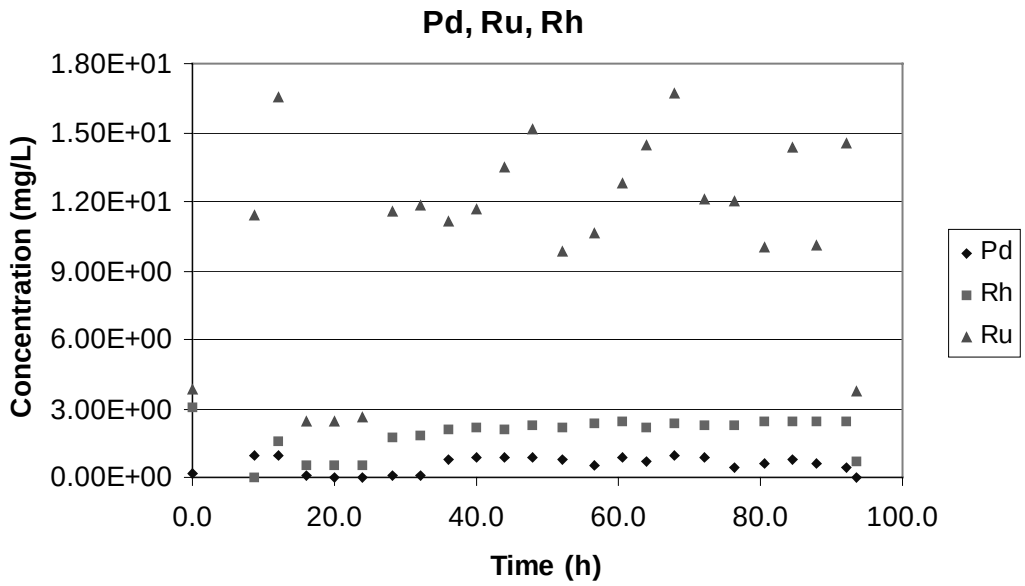

Figure 34. Pd, Rh, and Ru Concentrations Over Time.

For Pt and Hg, an examination of Figure 35 shows that while the Pt remains at a relatively steady concentration, the Hg shows a large drop in concentration over the first system turnover or so.

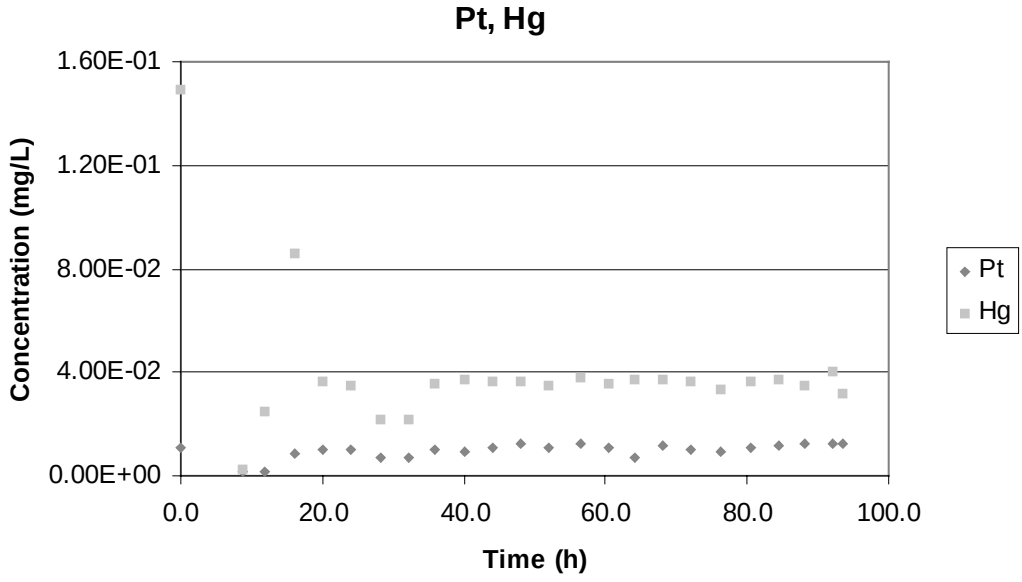

Figure 35. Pt and Hg Concentrations Over Time.

This drop in soluble mercury may indicate that soluble mercury(II) is being reduced to a catalytically active mercury(0) species which is the driving force for the benzene generation rate of 2.4 mg/(L•h).

5.0 CONCLUSIONS

This experiment successfully demonstrated the 5 main objectives to this task plan;

- The experiment demonstrated successful removal of cesium from the waste. The target DF was 10,000. During the entire experiment, the decontamination factor averaged 1.4 million after the equipment reached steady-state operation.

- The monosodium titanate successfully removed the actinides (Pu, U) from solution yielding a solution with an average alpha dose below 0.214 nCi/g after treatment versus a process requirement of 20 nCi/g.

- The experiment demonstrated successful removal of strontium from the waste. The target DF was 19.3 (Saltstone limits of 20 nCi/g). During the entire experiment, the DF averaged 45.6 after the equipment reached steady-state operation.

- Throughout the duration of the testing there was little hard evidence of foaming. We observed some small frothing in the sample lines before 45 °C was reached, and the interstage overflow tube between CSTR#1 and CSTR#2 plugged after 71 hours of operation.

- The slurry showed evidence of small amount of catalytic decomposition of the tetraphenylborate during the testing at 45 °C, giving a calculated benzene generation rate of 2.4 mg/(L•h).

Cesium DF was achieved. In fact, the ability of the system to remove cesium surpassed expectations, giving average DF values over the entire experiment[¥] 1.4 million for waste containing a high loading of cesium. Furthermore, this process does not appear to have a high dependency on temperature effects from 25 °C to 45 °C.

Regular MST additions successfully removed plutonium and uranium from the system. Plutonium removal achieved an average DF[§] of 126, and uranium achieved an average DF[§] of 2.36. Compared to the Saltstone limit of a total alpha activity of 20 nCi/g, on average the

[¥] This is calculated as a simple average and does not use the time=0 to 16 data points (before steady state).
[§] This is calculated as a simple average and does not use the time=0 data point (before steady state).

experiment achieved an activity of 0.214 nCi/g which corresponds to a alpha removal DF of 115. Temperature change from 25 °C to 45 °C had no apparent effect.

Regular MST additions also successfully removed Strontium from the system. Strontium removal achieved an average DF[§] of 45.6 nCi/g, compared to the requirement to meet Saltstone limits of a DF of 19.3.

The IIT B-52 antifoam appears to be successful, as no debilitating problems were noted that could be directly traced back to foaming. The only visual evidence of foaming behavior was that some of the slurries taken from the sample port were slightly frothy when exiting the port. Stable operations were maintained throughout the experiment, with the exception of an overflow plug from CSTR#1 to CSTR#2 after ~6 system turnovers (71 hours) into the test. This problem was quickly and completely alleviated through the use of a backup pump.
There was no evidence of TPB decomposition. At all times, in both tests, there were less than detectable amounts (<10 ppm) of TPB decomposition products; 3PB, 2PB, 1PB, or phenol. The increase in temperature caused no additional detectable decomposition of TPB.
While there was a decreasing amount of TPB in solution, this is not attributed to decomposition, but due to increasing sodium levels causing a decrease in TPB solubility levels.

6.0 QUALITY ASSURANCE

Laboratory Notebook WSRC-NB-2001-00030 (T. B. Peters) contains the experimental log for these experiments. Sample analysis data resides in Laboratory Notebook WSRC-NB-2001-00029 (T. B. Peters). Anderson recorded the data from examination of the nitrogen sparging efficiency in Laboratory Notebook WSRC-NB-2000-00214.

This work satisfies the requirements defined in the originating task plan [5] as well as those defined in the TR&C. The work complied with "Procedure for Real Waste Test of The Small Tank Precipitation Process" (Manual L12.1, Procedure IWT-OP-137, Rev. 1) or earlier versions as appropriate.

This report finalizes the work identified by Item 2.5 of "Applied Technology Integration Scope of Work Matrix for Small Tank TPB Precipitation (Demonstration Phase)," HLW-SDT-99-0353, Rev. 5, November 21, 2000.

7.0 ACKNOWLEGEMENTS

The authors thank the members of the various support groups that contributed to the success of this project. All members of the team worked many off-shift hours, including a large amount of uncompensated time, so as to complete the work in time for critical program decisions.

Mitch Peel and Mark Howell maintained the schedules that helped focus the efforts of the various team members. Their assistance help focus the chaos of the innumerable days into an efficient several month project. In hindsight, the apparent inefficient days merged into a rather efficient expenditure of resources and professional talents.

Tibor Horvath, assisted by Melissa McLain, coordinated the overall design efforts. Frederick Thompson and Narayan Bandyopadhyay developed the electrical drawings. Carolyn Nichols aided procurement and calibration issues. Larry Garosi coordinated the bulk of the electrical and mechanical fabrication efforts. Charlie (Pete) Price performed the largest portion of the electrical wiring, working weekends for nearly two months on this and a parallel effort for the program. Mike Restivo provided immense support in several critical areas including design details for tubing and vessel placements. Tim Steeper and Jerry Corbett greatly improved the brackets for holding the reaction vessels. Tommy McCoy provide specialized shop assistance on custom parts. Mike Armstrong, Jimmy Mills, and Vernon Bush performed much of the critical mechanical assembly. Brian Anderson and Jerry McCarty defined the shroud concept that allowed control of the oxygen content within the reaction vessels.

Larry Hill and Robert Chapman coordinated a number of facility support activities. Chapman supervised the fabrication and installation of a new mock-up deck to house the initial tests with a ventilation system, new electrical services, and nitrogen gas supplies. Undoubtedly, a large number of individuals contributed to these efforts unbeknownst to the authors.

The Shielded Cells Operations staff ensured the success of the experiments through their tireless efforts. Ron Blessing defined and implemented a number of refinements critical for success deployment in the remote-operating environment. Jane Johnson, Maurice Lee, and Debbie Sanders served as the operators for each experiment. David Healy also served as an operator and volunteered to shift assignments for the success of the program. Gary Hall repaired all the manipulators as needed on very short notice by working evenings and weekends. Babb Attaway, David Keel, and Carolyn Conley managed the extensive number of evolutions within the Shielded Cells in an incredibly smooth manner.

Hank Elder, Rick Fowler, Steve Subosits, and Fatina Washburn all served as part of the operating team of engineers overseeing the experiment. Fowler drafted the first version of the operating procedure. Lynn Nelson coordinated the efforts to issue the operating procedure. Hank Elder provided technical guidance on the sequence of operations for starting the experiments. Noel

Chapman, Bob Hinds, and Mark Geeting conducted a readiness review for operations that helped focus the work.

Mark Hubbard provided oversight to ensure the safe operation of the entire effort. He conducted safety reviews on short notice to help ensure completion of the work in a timely fashion. His suggestions protected us from many hazards and allowed the tired personnel to return home each day in an otherwise healthy state.

The work benfitted from the efforts of the talented staff that provided analytical support for the program. Mike Whittaker and Sharon Gleaton completed the atomic absorption spectroscopy work. Tom White and Annie Still performed the high-pressure liquid chromatography. Cici and David Diprete supervised the gamma spectroscopy. Beverly Burch performed the chemical digestions of samples to prepare for analysis.

Nancy Gregory, Minnie Hightower, Lin Thacker, Betty Croy, Shirley McCollum, and Kim Prettel each served as Technical Analysts for various tasks within the overall effort. Kim Prettel also supervised the procurement of the vast majority of the supplies and parts needed for the experiment. She likewise performed most of the photography including the numerous figures that occur within the document.

An effort of this magnitude succeeds due to the efforts of so many individuals. We apologize to those we forgot to mention in this list.

8.0 REFERENCES

1) D. D. Walker, M. J. Barnes, C. L. Crawford, R. F. Swingle, R. A. Peterson, M. S. Hay, and S. D. Fink, “Decomposition of Tetraphenylborate in Tank 48H”, WSRC-TR-96-0113, May 10, 1996.

2) R. A. Dimenna , H. H. Elder, J. R. Fowler, R. C. Fowler, M. V. Gregory, T. Hang, R. A. Jacobs, P. K. Paul, J. A. Pike, P. L. Rutland, F. G. Smith III, S. G. Subosits, G. A. Taylor, S. G. Campbell, Fatina A. Washburn, “Bases, Assumptions and Results for the Short List Alternatives,” WSRC-RP-99-00006, Rev 1. October, 1999.

3) R. A. Peterson and J. O. Burgess, “The Demonstration of Continuous Stirred Tank Reactor Operations with High Level Waste,” WSRC-TR-99-00345, Rev. 1, February 15, 2000.

4) H. H. Elder, “Small Tank Tetraphenylborate Precipitation Real Waste Test”, HLW-STD-TTR-2000-00011, September 20, 2000.

5) T. B. Peters and R. A. Peterson, “Task Technical and Quality Assurance Plan for Demonstration of Continuous Stirred Tank Reactor Operations with High Level Waste,” WSRC-RP-2000-00884, October 16, 2000.

6) Procedure for Real Waste test of the Small Tank Precipitation Process, IWT-OP-137, Rev 3.

7) M. A. Baich, D. P. Lambert, P. R. Monson, "Laboratory Scale AntiFoam Studies for the STTPB Process", WSRC-TR-2000-00261, October 24, 2000.

8) D. R. Best, T. L. White, "IIT B-52 Antifoam Analytical Technique Using High Performance Liquid Chromatography and a Evaporative Light Scattering Detector", WSRC-TR-2001-00135, March 16, 2001.

9) WSRC 1S Savannah River Site Waste Acceptance Criteria Manual, Procedure 4.01, "Acceptance Crieria for Aqueous Waste Sent to the Z Area Saltstone Production Facility", Rev. 2, June 19, 1998.

10) M. J. Barnes, B. B. Anderson, T. L. White, K. B. Martin, "Tetraphenylborate Decomposition Testing Using Actual Savannah River Site High Level Waste", WSRC-TR-2001-00251, May 3, 2001.

11) T. B. Calloway, M. A. Baich, D. P. Lambert, "Fate of IIT B-52 Antifoam Agent Across the Small Tank Tetraphenylborate Process", WSRC-TR-2001-00102, May, 2001.

12) M. J. Barnes, J. F. McGlynn, R. F. Swingle, D. D. Walker, "ITP and Late Wash Salt Solution Foaming Characteristics", WSRC-TR-94-152, July 14, 1994.

13) M. J. Barnes, R. A. Peterson, S. R. White, "Cesium Removal Kinetics and Equilibrium: Precipitation Kinetics", WSRC-TR-99-00325, Rev. 0, September 8, 1999.

14) D. J. McCabe, "Cesium, Potassium, and Sodium Tetraphenylborate Solubility in Salt Solution", WSRC-TR-96-0384, Rev. 0, December 16, 1996.

15) D. T. Hobbs, R. L. Pulmano, "Phase IV Testing of Monosodium Titanate Adsorbtion With Radioactive Waste", WSRC-TR-99-00286, Rev. 0, September 3, 1999.

APPENDIX 1: OXYGEN CONTROL

ADS was tasked with making headspace oxygen measurements for CSTRs before the real waste test itself. ADS utilized the Ocean Optics FOXY fiber optic oxygen sensor and newest version of the OOISensors software to record oxygen content as percent oxygen as a function of time. The overall goal of the work is to determine the effectiveness of the nitrogen headspace purge used in the mock up test to reduce and maintain an oxygen concentration below 4.5% in the headspace above the CSTR reaction space. CSTR headspaces were purged with a maximum flow rate of 30 cc/min. from an ultra high purity nitrogen tank. The two CSTR vessels are in sequence, with CSTR 1 overflow to CSTR 2. CSTR 2 was more amenable to the placement of a small fiber optic probe due to the large area above the CSTR top and below the CSTR mandrel, which served to secure the various feed and service tubes such that they would not touch the CSTR itself. Therefore, all measurements were performed in the headspace or liquid volume of CSTR 2. The oxygen sensor was calibrated in air and nitrogen prior to each introduction into the CSTR 2 headspace. Based on previous calibrations, we made the assumption that the calibration would not change significantly (2-3%) if the probe were calibrated in gas and then introduced into liquid. Several runs exhibited drift on the oxygen measurements, and the presence of a bright halogen lamp behind the rig complicated that calibration in some instances, introducing a 3-4% bias over the course of the experiment. This data presented here are to provide a measure of the effectiveness of the purge, and the steps taken to ensure adequate purge geometry and flow rates after subsequent measurements indicated inadequate purge.

Initial measurements were made on 2/22/01 where the FOXY probe was placed in the headspace of CSTR 2 and both CSTR 1 and 2 mass flow controlled nitrogen purges were activated at 15 cc/min. The data collected on this day are shown in Figure A. The purge was changed to 30 cc/min. at 11:09 a.m., and a small downward trend in oxygen concentration is noticed. However, the expected decrease in oxygen to low percent levels did not occur, and it was established that the purge of the headspace was not sufficient due to the large exchange of the unsealed headspace with atmosphere. The system appeared to reach equilibrium at around 18%. The increase in O_2 content at 12:37 p.m. is due to the removal of the probe to atmosphere to check the calibration, which appeared to be stable as air contains 20.95% oxygen.

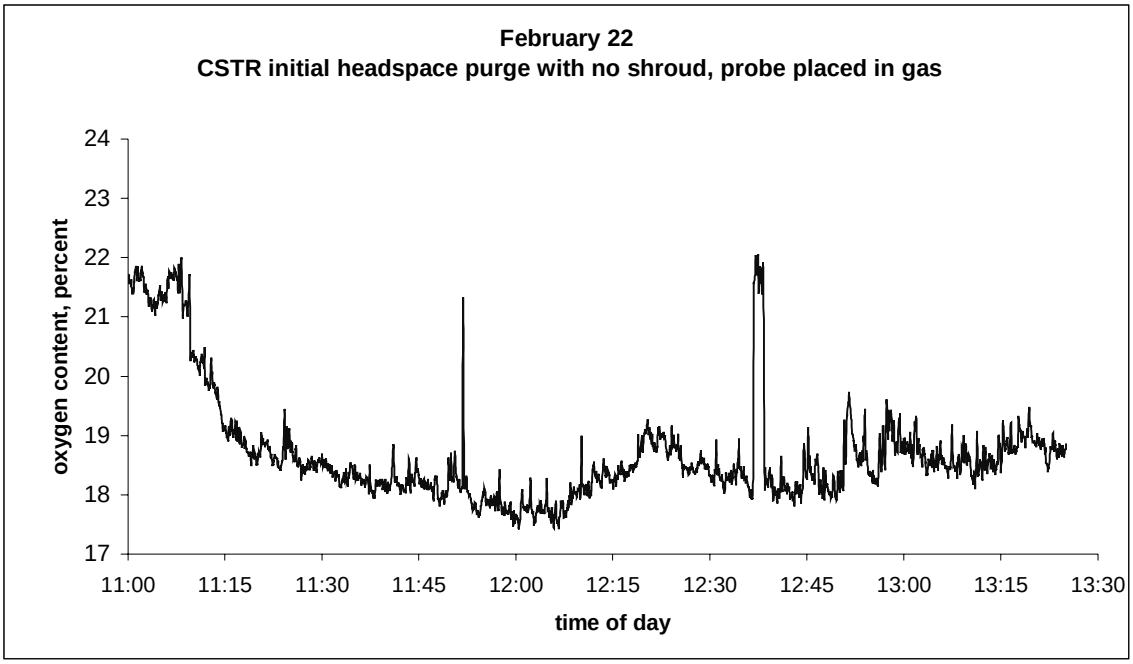

Figure A. CSTR initial headspace oxygen measurement on 2/22/01 shows that the initial purge specifications are not sufficient to render the headspace anoxic.

The CSTR headspace purge rate could not be changed due to design criteria for the CSTRs. It was postulated that the headspace purge (at 30 cc/min.) could be successful if the atmosphere above the CSTR vessel were purged at a higher rate than the CSTR, which would in theory prevent the exchange of atmospheric oxygen with the CSTR headspaces. Therefore, a flexible shroud (Parafilm pressed against the sides of the CSTR edges) was attached to the space above the CSTR top and this space purged under high nitrogen flow (several liters per minute) directly from a ¼ " o.d. hard plastic tube attached to the nitrogen tank via a Swage-loc tee. Figure B shows the successful results of this exterior purge.

The sensor was also placed into the liquid space of CSTR with the shroud installed. The liquid reached between 5 and 12% oxygen, representing an oxygen content reduction from air saturation of between 50 and 75%. Although the liquid appeared to not reach anoxic levels, sparging the liquid was not an option due to the foaming properties of either the simulant or real waste slurries. Figure C shows the liquid oxygen content as a function of time as the CSTR feeds are turned on.

Similar experiments were performed with an engineered shroud made out of Saran Wrap and secured to the CSTR via tie wraps in a configuration that would be implemented in the cells. The external (shroud) space has nitrogen plumbed in via hard tubing, gas rotameters (0-20 standard cubic feet per hour (SCFH)) and check valves with quick connects. The feeds into the CSTRs

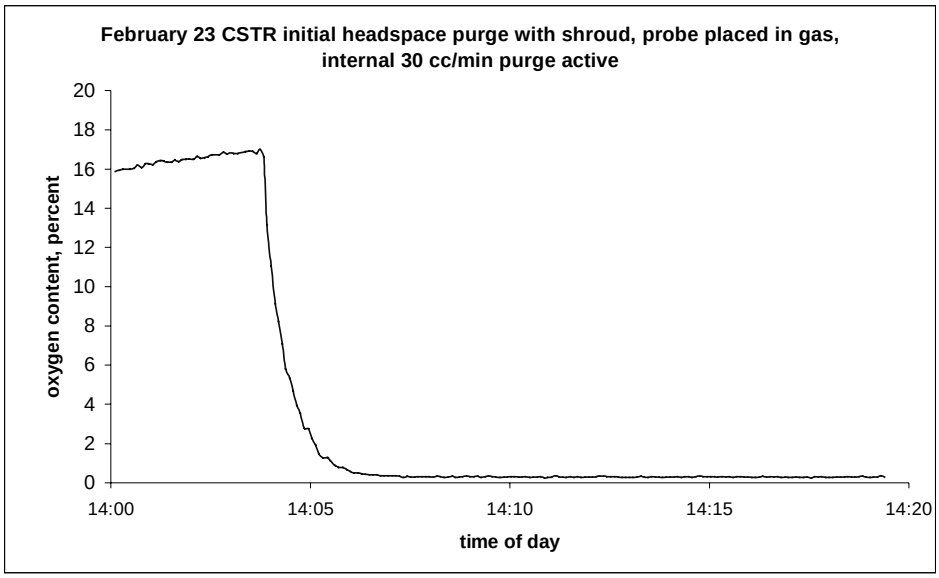

Figure B. Oxygen concentration of CSTR 2 headspace with external shroud purge at several liters per minute. External purge activated at 2:04 p.m., and the oxygen content in the CSTR rapidly dropped to less than 1%, proving the viability of the shroud for keeping the CSTR headspaces anoxic

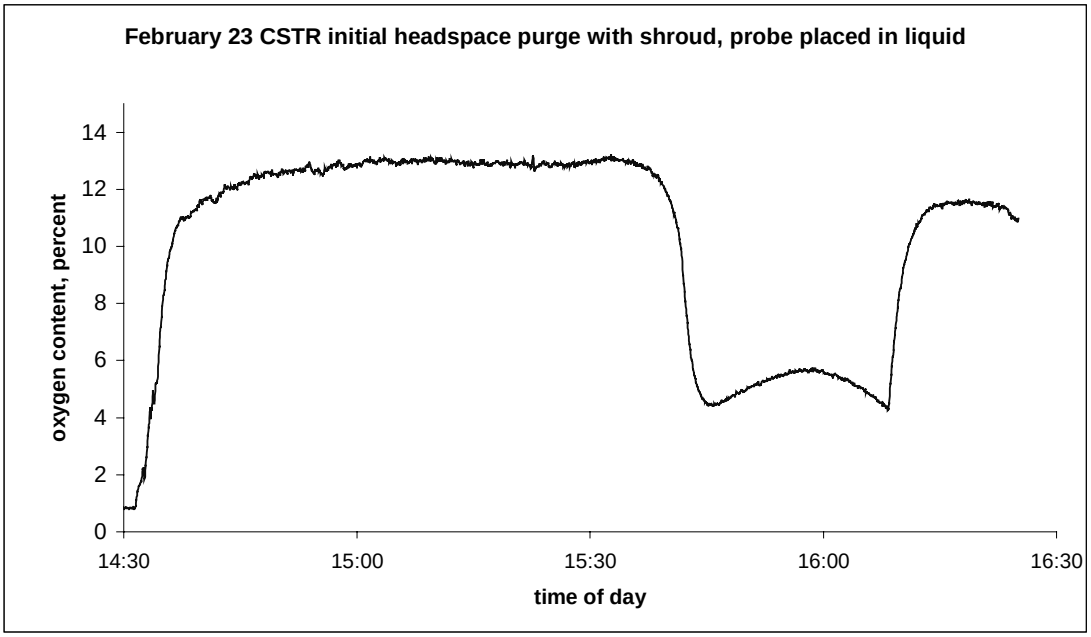

Figure C. CSTR 2 liquid oxygen content with shroud

were made with 1/8" o.d. Tygon tubing. The test was initialized with no flow, and the oxygen was measured inside the headspace at 24.77%, which is 2.8% higher than the calibration point of room air at 21.9%. This bias is attributable to the stray light entering the fiber optic probe tip

during the room air calibration step. We decided to keep the sensor in the CSTR headspace and run the experiment in the presence of this bias, which was cross-checked and verified at the end of the experiment by placing the sensor in pure nitrogen and then room air, this time shielded from the bright halogen lamp located behind the CSTR setup.

After the sensor was placed into the headspace, the internal headspace flow was activated at 30 cc/min and the agitators turned on. After equilibrium was quickly reached with essentially no change in the oxygen content, the shroud purge was switched on, with the rotameters exhibiting inconsistent flow characteristics. As can be seen in Figure D, the system reached a steady state of 18% oxygen, and this was due to the fact that the CSTR system had only one of the two available shroud purge lines active. After this, the line was activated and the oxygen continued to trend down. However, it appeared that the check valves were hindering the flow rate excessively, and these were then removed. The system was then purged, sans check valves, using the rotameters set to their maximum flow settings. The meters have a maximum scale of 20 SCFH, and this corresponds to 9.4 L/min flow. At maximum flow, with the pressure regulator set at 5 psi, the rotameters read between 2 and 4 SCFH, which corresponds to 1-2 L/min flow split between the two CSTR's. It is estimated that the shroud volume above CSTR 2 is about .5 L, and the volume above CSTR 2 is about half of that, or .25 L. Therefore, the flow rate with the rotameters set at maximum flow is sufficient to exchange the shroud volume 1-2 times per minute. It appears that the steady state for the configurations without check valves is approximately 5%, which corresponds to ~2.5% oxygen when corrected for the initial bias. Thus, at maximum flow provided by the regulator, the equilibrium is reached which corresponds to 2.5% oxygen content in the headspace above the CSTRs. Upon inspection of the data, it appears that the rate of oxygen removal with and without the check valves in-line is comparable, and therefore our initial concerns that the check valves may be impeding the flow were unfounded. We postulated that the 1/8" Tygon tubing was creating a restriction orifice, preventing sufficient flow to the shrouds.

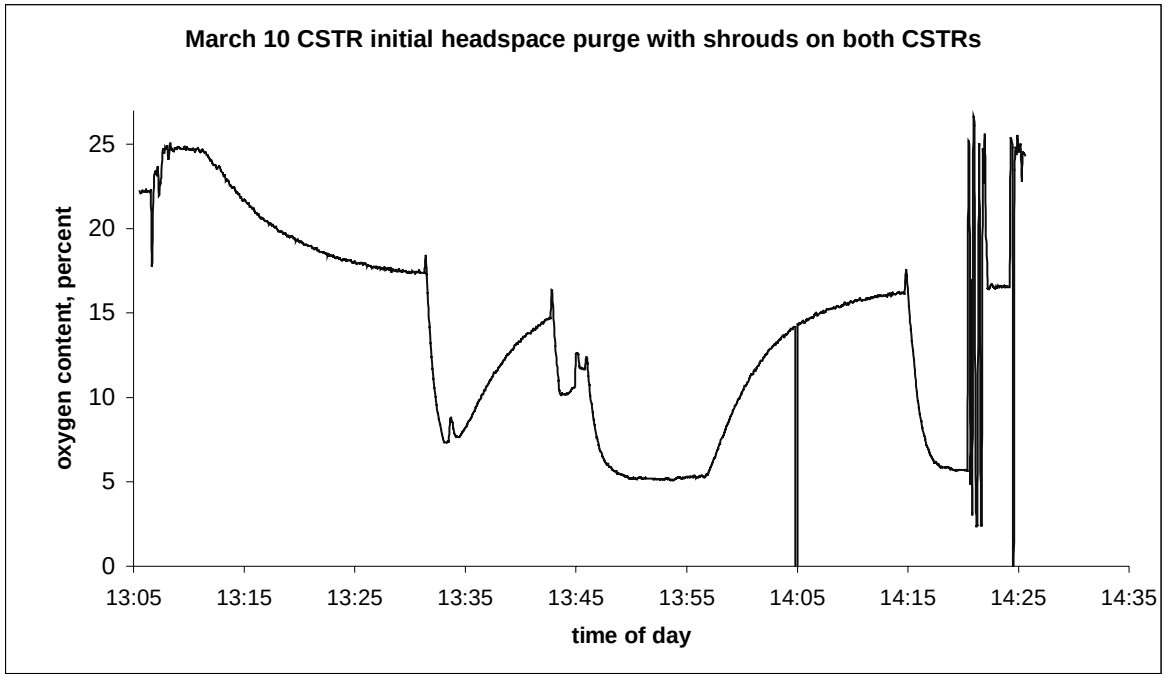

Figure D. March 10, 2001 Engineered Shroud Purge Test.

After this test the check valves and rotameters were reinstalled along with larger tubing to the CSTR shrouds and a second purge test run with both shrouds (new) on and purged with the rotameters set at 10 scfm. Figure E shows the results of this test, indicating that the larger tubing allows sufficient flow rate for complete removal of oxygen from the CSTR headspace and shrouds. It is clear that the system rapidly approached anoxic in the headspace of CSTR 2 proving that the limiting factor in the previous tests was the restriction orifice caused by the small diameter tubing.

On March 12, 2001, the sensor was calibrated and placed into the headspace of CSTR 2 as before and data collected over the course of the experiment. Figure F is provided to demonstrate the

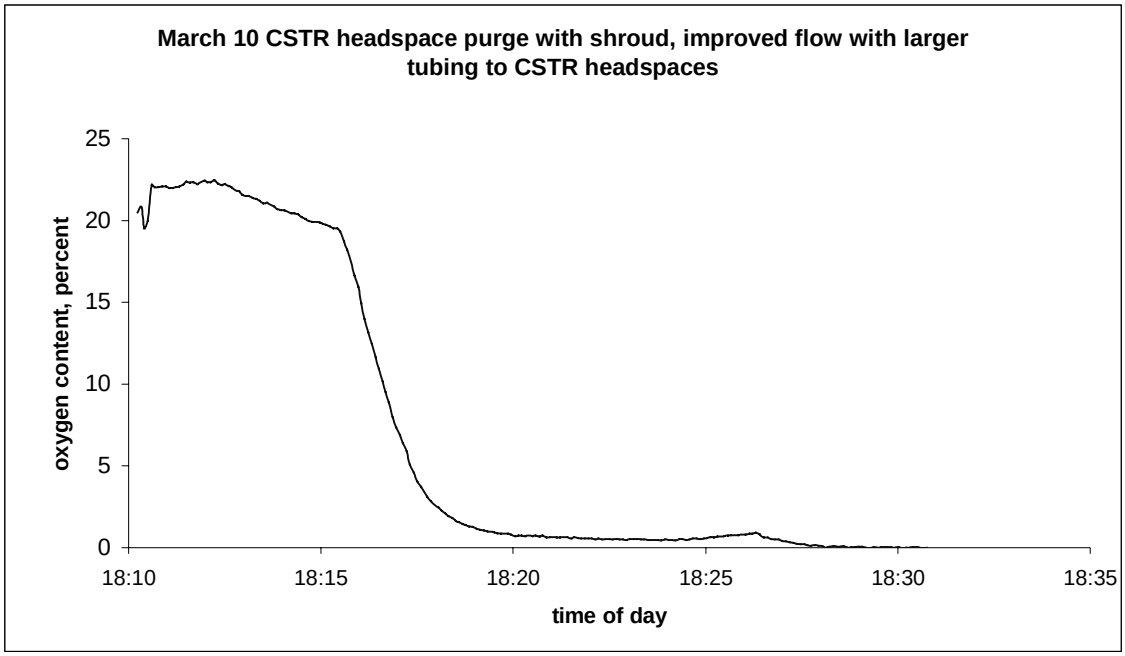

Figure E. Second shroud test on March 10 with larger tubing to shroud purge lines. The CSTR 30 cc/min. purges were switched on at 6:10 p.m., and then at 6:15 p.m. the shroud purge was turned on at 10 scfm, resulting in a rapid reduction of the oxygen concentration to below 1%.

initial oxygen depletion as the test is begun. The sensor was placed into the system at 7:30 a.m., however the test did not start until 9:30 a.m., and this provides a good measure of the sensor stability for those two hours, where the sensor exhibited minimal drift. Once the purges were activated at 10:00 a.m., the headspace of CSTR 2 rapidly went to less than 1% oxygen. The rise on oxygen level at approximately 6:00 p.m. is due to the depletion of nitrogen in the tank, necessitating the tank replacement with a fully charged tank.

In summation, the CSTRs can be kept under anoxic conditions through the use of a two tiered nitrogen purge system using a total of 20 SCFH per CSTR.

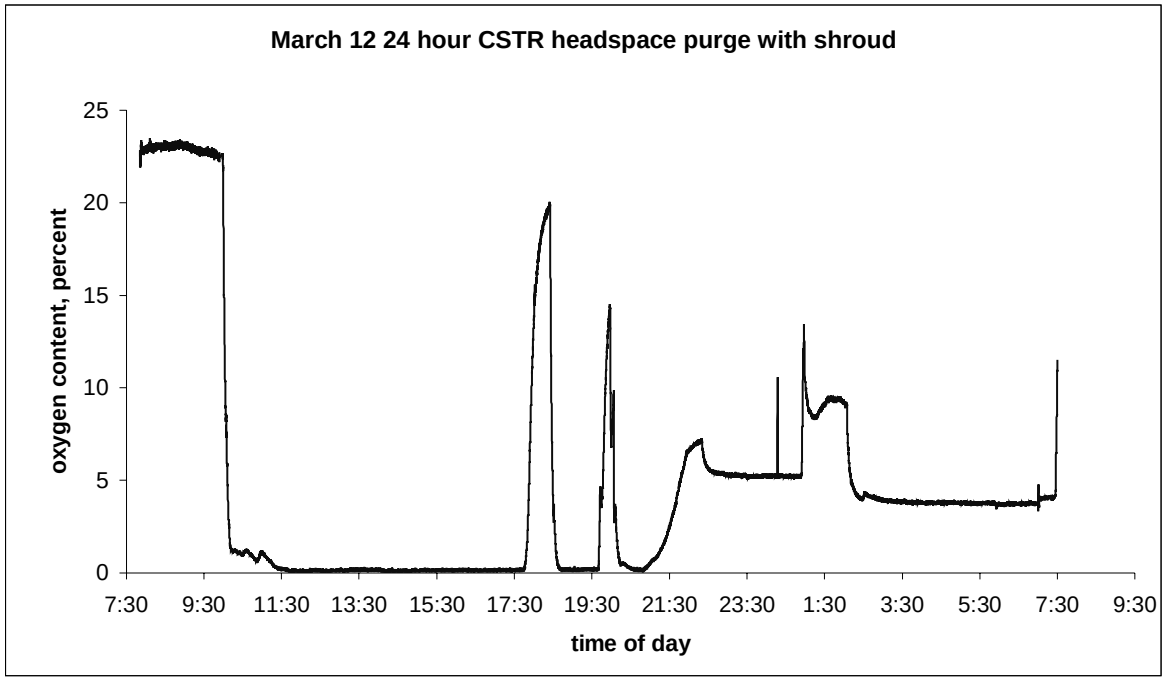

Figure F. CSTR 24 hour test oxygen levels. The system rapidly reached <1% oxygen after the purge lines were activated.

Appendix 2. Design of Extraction Tool To Remove Recessed Pins

The final adjustments and tweaking to the equipment to be installed in the high activity cells was done by 3/15/01. The equipment was installed into the cells on 3/16/01. Assembly of the different parts (main rack, feed rack, receipt rack, chillers, tubes, and cables) took from 3/16/01 to 3/17/01.

The real waste test was scheduled to start on 3/18/01, but it was found that incorrect assembly of the 19 pin cable head caused three of the pins to be recessed into the plug head (Figure G). The three recessed pins prevented operation of several of the pumps. Fortunately, Shielded Cells personnel were able to design and construct a special tool to extract the recessed pins (Figure H).

Figure G. Recessed Pins Prevent Normal Operations.

The tool worked perfectly and in a matter of an hour or so the pins were returned to their proper position. The cable head has then installed correctly and all functions returned. Thanks to this simple, yet effective tool, a much longer delay was avoided (3+ days estimated). Only 24 hours had been lost, and the test formally started on late 3/19/01.

Figure H. The GPR[#] Supertool.

[#] GPR stands for **G**ary Hall, **P**ete Bogart, and **R**on Blessing.

Appendix 3. Tabulated Data for the Real Waste Test.

Table A. Sodium and Potassium Concentrations Over Time.

Sample ID	Time (h)	Potassium (mM)	Sodium (M)
0-0-STTP-1	0.0	82.35	10.2
1-8-STTP-1	8.8	8.2628	4.49
2-12-STTP-1	12.0	5.9898	4.56
3-16-STTP-1	16.0	3.715	4.44
4-20-STTP-1	20.0	< 0.00345	4.61
5-24-STTP-1	24.0	< 0.00345	4.62
6-28-STTP-1	28.3	< 0.00345	4.63
7-32-STTP-1	32.3	< 0.00345	4.71
8-36-STTP-1	36.0	< 0.00345	4.70
9-40-STTP-1	40.0	< 0.00345	4.70
10-44-STTP-1	44.0	< 0.00345	4.84
11-48-STTP-1	48.0	< 0.00416	5.06
12-52-STTP-1	52.0	< 0.00373	4.48
13-56-STTP-1	56.5	< 0.00402	4.39
14-60-STTP-1	60.5	0.012	4.36
15-64-STTP-1	64.0	< 0.00345	4.43
16-68-STTP-1	68.0	< 0.00345	4.45
17-72-STTP-1	72.0	< 0.00345	4.46
18-76-STTP-1	76.3	< 0.00345	4.90
19-80-STTP-1	80.5	< 0.00422	4.87
20-84-STTP-1	84.5	0.00540	4.84
21-88-STTP-1	88.0	< 0.00345	4.83
22-92-STTP-1	92.0	< 0.00345	4.88
A-93.5-STTP-1	93.5	< 0.00345	5.13

Table B. Strontium Activity Over Time.

Sample ID	Time (h)	Strontium (nCi/g)
0-0-STTP-5	0.0	772
1-8-STTP-5	8.8	57.8
2-12-STTP-5	12.0	41.1
3-16-STTP-5	16.0	27.2
4-20-STTP-5	20.0	22.6
5-24-STTP-5	24.0	20.8
6-28-STTP-5	28.3	19.7
7-32-STTP-5	32.3	20.4
8-36-STTP-5	36.0	18.5
9-40-STTP-5	40.0	17.0
10-44-STTP-5	44.0	19.4
11-48-STTP-5	48.0	17.0
12-52-STTP-5	52.0	17.3
13-56-STTP-5	56.5	16.0
14-60-STTP-5	60.5	11.9
15-64-STTP-5	64.0	10.9
16-68-STTP-5	68.0	10.6
17-72-STTP-5	72.0	10.0
18-76-STTP-5	76.3	13.2
19-80-STTP-5	80.5	14.5
20-84-STTP-5	84.5	15.7
21-88-STTP-5	88.0	17.5
22-92-STTP-5	92.0	16.5
A-93.5-STTP-5	93.5	21.5

Table C. Uranium Activity Over Time.

Sample ID	Time (h)	U-233 Act. nCi/g	U-235 Act. nCi/g	U-238 Act. nCi/g	Total U Act. nCi/g
0-0-STTP-3	0.0	2.58E-02	3.06E-04	9.94E-04	2.71E-02
1-8-STTP-3	8.8	< 1.37E-02	< 3.06E-06	4.28E-04	1.41E-02
2-12-STTP-3	12.0	< 1.37E-02	< 3.06E-06	4.35E-04	1.42E-02
3-16-STTP-3	16.0	1.87E-02	1.77E-04	4.68E-04	1.94E-02
4-20-STTP-3	20.0	2.50E-02	1.80E-04	4.57E-04	2.57E-02
5-24-STTP-3	24.0	1.64E-02	1.77E-04	4.64E-04	1.71E-02
6-28-STTP-3	28.3	1.37E-02	4.01E-05	4.34E-07	1.37E-02
7-32-STTP-3	32.3	1.38E-02	3.82E-05	4.86E-07	1.39E-02
8-36-STTP-3	36.0	1.39E-02	2.01E-04	4.23E-04	1.45E-02
9-40-STTP-3	40.0	1.54E-02	1.92E-04	4.20E-04	1.61E-02
10-44-STTP-3	44.0	1.47E-02	1.99E-04	4.27E-04	1.54E-02
11-48-STTP-3	48.0	1.47E-02	1.99E-04	4.26E-04	1.53E-02
12-52-STTP-3	52.0	1.47E-02	1.97E-04	4.42E-04	1.53E-02
13-56-STTP-3	56.5	2.06E-02	2.11E-04	4.48E-04	2.12E-02
14-60-STTP-3	60.5	1.50E-02	1.89E-04	4.18E-04	1.56E-02
15-64-STTP-3	64.0	2.55E-02	1.67E-04	3.35E-04	2.60E-02
16-68-STTP-3	68.0	2.07E-02	1.49E-04	3.42E-04	2.12E-02
17-72-STTP-3	72.0	< 1.37E-04	1.55E-04	3.50E-04	6.43E-04
18-76-STTP-3	76.3	1.54E-02	1.80E-04	3.82E-04	1.60E-02
19-80-STTP-3	80.5	1.75E-02	1.74E-04	3.80E-04	1.81E-02
20-84-STTP-3	84.5	1.56E-02	1.79E-04	3.85E-04	1.62E-02
21-88-STTP-3	88.0	1.95E-02	1.79E-04	4.01E-04	2.01E-02
22-92-STTP-3	92.0	1.35E-02	1.92E-04	4.01E-04	1.41E-02
A-93.5-STTP-3	93.5	1.62E-02	1.59E-04	4.15E-04	1.68E-02

Table D. Plutonium Activity Over Time.

Sample ID	Time (h)	Pu-238 (dpm/mL)	Pu-238 DF	Pu-239/240 (dpm/mL)	Pu238 Act nCi/g	Pu239/240Act nCi/g	Total Pu Act nCi/g
0-0-STTP-4	0.0	63883		1857	23.980105	0.6970720	24.677177
1-8-STTP-4	8.8	1030	62	< 149.00	0.3866366	0.0559309	0.4425675
2-12-STTP-4	12.0	734	87	221	0.2755255	0.0829579	0.3584834
3-16-STTP-4	16.0	530	121	3.1	0.1989489	0.0011636	0.2001126
4-20-STTP-4	20.0	544	117	2.06	0.2042042	0.0007732	0.2049774
5-24-STTP-4	24.0	702	91	4.63	0.2635135	0.0017379	0.2652515
6-28-STTP-4	28.3	615	104	2.15	0.2308558	0.0008070	0.2316629
7-32-STTP-4	32.3	601	106	< 0.908	0.2256006	0.0003408	0.2259414
8-36-STTP-4	36.0	558	114	2.73	0.2094594	0.0010247	0.2104842
9-40-STTP-4	40.0	574	111	< 0.827	0.2154654	0.0003104	0.2157759
10-44-STTP-4	44.0	582	110	4.73	0.2184684	0.0017755	0.2202439
11-48-STTP-4	48.0	705	91	1.95	0.2646396	0.0007319	0.2653716
12-52-STTP-4	52.0	551	116	< 1.08	0.2068318	0.0004054	0.2072372
13-56-STTP-4	56.5	530	121	3.82	0.1989489	0.0014339	0.2003828
14-60-STTP-4	60.5	483	132	10.4	0.1813063	0.0039039	0.1852102
15-64-STTP-4	64.0	221	289	< 1.00	0.0829579	0.0003753	0.0833333
16-68-STTP-4	68.0	296	216	15.0	0.1111111	0.0056306	0.1167417
17-72-STTP-4	72.0	263	243	2.86	0.0987237	0.0010735	0.0997972
18-76-STTP-4	76.3	321	199	3.34	0.1204954	0.0012537	0.1217492
19-80-STTP-4	80.5	296	216	1.58	0.1111111	0.0005930	0.1117042
20-84-STTP-4	84.5	524	122	72.5	0.1966966	0.0272147	0.2239114
21-88-STTP-4	88.0	308	207	3.50	0.1156156	0.0013138	0.1169294
22-92-STTP-4	92.0	317	202	< 1.01	0.1189939	0.0003791	0.1193731
A-93.5-STTP-4	93.5	311	205	4.41	0.1167417	0.0016554	0.1183971

Table E. Total Alpha Activity (U + Pu) Over Time.

Sample ID	Time (h)	Total Alpha nCi/g
0-0-STTP-3	0.0	2.47E+01
1-8-STTP-3	8.8	4.57E-01
2-12-STTP-3	12.0	3.73E-01
3-16-STTP-3	16.0	2.20E-01
4-20-STTP-3	20.0	2.31E-01
5-24-STTP-3	24.0	2.82E-01
6-28-STTP-3	28.3	2.45E-01
7-32-STTP-3	32.3	2.40E-01
8-36-STTP-3	36.0	2.25E-01
9-40-STTP-3	40.0	2.32E-01
10-44-STTP-3	44.0	2.36E-01
11-48-STTP-3	48.0	2.81E-01
12-52-STTP-3	52.0	2.23E-01
13-56-STTP-3	56.5	2.22E-01
14-60-STTP-3	60.5	2.01E-01
15-64-STTP-3	64.0	1.09E-01
16-68-STTP-3	68.0	1.38E-01
17-72-STTP-3	72.0	1.00E-01
18-76-STTP-3	76.3	1.38E-01
19-80-STTP-3	80.5	1.30E-01
20-84-STTP-3	84.5	2.40E-01
21-88-STTP-3	88.0	1.37E-01
22-92-STTP-3	92.0	1.33E-01
A-93.5-STTP-3	93.5	1.35E-01

Table F. Total Soluble Boron Over Time

LIMS #	Sample ID	Time (h)	Boron (mg/L)
3-160652	0-0-STTP-7	0.0	
3-160655	1-8-STTP-7	8.8	< 0.375
3-160656	2-12-STTP-7	12.0	< 0.375
3-160657	3-16-STTP-7	16.0	73.6
3-160658	4-20-STTP-7	20.0	78.5
3-160659	5-24-STTP-7	24.0	80.5
3-160671	6-28-STTP-7	28.3	81.1
3-160672	7-32-STTP-7	32.3	81.4
3-160738	8-36-STTP-7	36.0	81.5
3-160739	9-40-STTP-7	40.0	81.9
3-160740	10-44-STTP-7	44.0	80.7
3-160741	11-48-STTP-7	48.0	80.0
3-160799	12-52-STTP-7	52.0	81.5
3-160800	13-56-STTP-7	56.5	82.0
3-160801	14-60-STTP-7	60.5	81.6
3-160802	15-64-STTP-7	64.0	81.9
3-160803	16-68-STTP-7	68.0	82.9
3-160804	17-72-STTP-7	72.0	82.6
3-160835	18-76-STTP-7	76.3	83.4
3-160836	19-80-STTP-7	80.5	83.3
3-160837	20-84-STTP-7	84.5	83.9
3-160838	21-88-STTP-7	88.0	83.8
3-160839	22-92-STTP-7	92.0	83.8
3-161339	A-93.5-STTP-7	93.5	84.4

Table G. ICP-MS of Various Elements Over Time.

Sample ID	Time (h)	Zr (mg/L)	Tc-99 (mg/L)	Mo (mg/L)
0-0-STTP-3	0.0	8.56E-01	1.75E+01	1.05E+02
1-8-STTP-3	8.8	< 1.07E-02	2.06E+01	6.67E+01
2-12-STTP-3	12.0	< 1.07E-02	2.06E+01	6.56E+01
3-16-STTP-3	16.0	< 4.38E-04	1.16E+01	7.42E+01
4-20-STTP-3	20.0	1.07E-01	1.21E+01	5.86E+01
5-24-STTP-3	24.0	1.63E-01	1.21E+01	5.90E+01
6-28-STTP-3	28.3	1.72E-01	2.94E+01	7.43E+01
7-32-STTP-3	32.3	2.96E-01	2.97E+01	7.74E+01
8-36-STTP-3	36.0	9.50E-02	1.03E+01	8.42E+01
9-40-STTP-3	40.0	2.89E-02	1.09E+01	8.67E+01
10-44-STTP-3	44.0	8.40E-02	1.08E+01	8.67E+01
11-48-STTP-3	48.0	7.61E-02	1.16E+01	9.13E+01
12-52-STTP-3	52.0	3.08E-02	1.07E+01	8.66E+01
13-56-STTP-3	56.5	9.91E-02	1.17E+01	9.22E+01
14-60-STTP-3	60.5	2.45E-02	1.18E+01	9.32E+01
15-64-STTP-3	64.0	2.20E-02	1.10E+01	9.00E+01
16-68-STTP-3	68.0	4.49E-02	1.16E+01	9.34E+01
17-72-STTP-3	72.0	6.10E-02	1.12E+01	8.82E+01
18-76-STTP-3	76.3	8.70E-02	1.11E+01	8.76E+01
19-80-STTP-3	80.5	2.94E-02	1.12E+01	9.22E+01
20-84-STTP-3	84.5	5.04E-02	1.16E+01	9.43E+01
21-88-STTP-3	88.0	2.58E-02	1.15E+01	9.50E+01
22-92-STTP-3	92.0	1.01E-01	2.62E+01	9.35E+01
A-93.5-STTP-3	93.5	< 1.81E-03	1.72E+01	1.02E+02

Table G, Continued.

Sample ID	Time (h)	Ag (mg/L)	Pd (mg/L)	Rh (mg/L)
0-0-STTP-3	0.0	4.97E-02	1.44E-01	3.06E+00
1-8-STTP-3	8.8	8.02E-02	9.75E-01	< 1.27E-02
2-12-STTP-3	12.0	6.85E-02	9.92E-01	1.53E+00
3-16-STTP-3	16.0	2.69E-02	6.87E-02	4.81E-01
4-20-STTP-3	20.0	1.62E-02	2.40E-02	4.99E-01
5-24-STTP-3	24.0	0.00E+00	2.62E-02	4.96E-01
6-28-STTP-3	28.3	1.07E-01	1.08E-01	1.75E+00
7-32-STTP-3	32.3	3.00E-02	1.04E-01	1.79E+00
8-36-STTP-3	36.0	4.83E-02	8.22E-01	2.12E+00
9-40-STTP-3	40.0	4.27E-02	8.60E-01	2.16E+00
10-44-STTP-3	44.0	3.94E-02	8.57E-01	2.12E+00
11-48-STTP-3	48.0	3.09E-02	8.37E-01	2.25E+00
12-52-STTP-3	52.0	2.72E-02	8.02E-01	2.17E+00
13-56-STTP-3	56.5	3.32E-02	5.00E-01	2.33E+00
14-60-STTP-3	60.5	3.67E-02	8.70E-01	2.42E+00
15-64-STTP-3	64.0	5.08E-02	6.63E-01	2.20E+00
16-68-STTP-3	68.0	7.02E-02	9.52E-01	2.33E+00
17-72-STTP-3	72.0	3.13E-02	8.82E-01	2.26E+00
18-76-STTP-3	76.3	2.80E-02	4.32E-01	2.30E+00
19-80-STTP-3	80.5	2.81E-02	6.07E-01	2.40E+00
20-84-STTP-3	84.5	3.92E-02	8.00E-01	2.43E+00
21-88-STTP-3	88.0	5.21E-02	6.12E-01	2.40E+00
22-92-STTP-3	92.0	3.85E-02	4.73E-01	2.42E+00
A-93.5-STTP-3	93.5	2.58E-02	3.50E-02	6.96E-01

Table G, Continued.

Sample ID	Time (h)	Ru (mg/L)	Cd (mg/L)	Sn (mg/L)
0-0-STTP-3	0.0	3.85E+00	3.96E-01	3.47E+00
1-8-STTP-3	8.8	1.14E+01	< 2.72E-02	6.74E+00
2-12-STTP-3	12.0	1.65E+01	< 2.72E-02	4.49E+00
3-16-STTP-3	16.0	2.46E+00	2.86E-01	2.59E+00
4-20-STTP-3	20.0	2.41E+00	2.78E-01	2.61E+00
5-24-STTP-3	24.0	2.58E+00	2.83E-01	2.67E+00
6-28-STTP-3	28.3	1.16E+01	1.99E-01	1.46E+01
7-32-STTP-3	32.3	1.18E+01	7.90E-02	1.46E+01
8-36-STTP-3	36.0	1.11E+01	1.68E-01	5.74E+00
9-40-STTP-3	40.0	1.16E+01	3.84E-01	5.87E+00
10-44-STTP-3	44.0	1.35E+01	1.94E-01	5.83E+00
11-48-STTP-3	48.0	1.51E+01	2.38E-01	6.19E+00
12-52-STTP-3	52.0	9.86E+00	6.38E-01	6.10E+00
13-56-STTP-3	56.5	1.06E+01	5.81E-01	6.42E+00
14-60-STTP-3	60.5	1.28E+01	2.67E-01	6.39E+00
15-64-STTP-3	64.0	1.44E+01	5.32E-01	6.14E+00
16-68-STTP-3	68.0	1.67E+01	8.54E-01	6.31E+00
17-72-STTP-3	72.0	1.21E+01	5.07E-01	6.04E+00
18-76-STTP-3	76.3	1.20E+01	5.73E-01	6.07E+00
19-80-STTP-3	80.5	9.99E+00	8.30E-01	5.95E+00
20-84-STTP-3	84.5	1.44E+01	5.62E-01	5.96E+00
21-88-STTP-3	88.0	1.01E+01	2.12E-01	6.06E+00
22-92-STTP-3	92.0	1.45E+01	5.76E-01	6.18E+00
A-93.5-STTP-3	93.5	3.76E+00	3.44E-01	5.19E+00

Table G, Continued.

Sample ID	Time (h)	W (mg/L)	Re (mg/L)	Ir (mg/L)
0-0-STTP-3	0.0	8.81E-01	1.22E-02	2.28E-03
1-8-STTP-3	8.8	8.55E-01	< 1.87E-03	< 5.00E-04
2-12-STTP-3	12.0	7.83E-01	< 1.87E-03	< 5.00E-04
3-16-STTP-3	16.0	6.95E-01	7.04E-03	3.18E-03
4-20-STTP-3	20.0	6.77E-01	6.95E-03	2.88E-03
5-24-STTP-3	24.0	6.91E-01	6.44E-03	2.99E-03
6-28-STTP-3	28.3	5.40E-01	5.09E-03	2.06E-03
7-32-STTP-3	32.3	5.34E-01	4.64E-03	2.08E-03
8-36-STTP-3	36.0	8.18E-01	8.04E-03	3.38E-03
9-40-STTP-3	40.0	8.06E-01	6.86E-03	3.00E-03
10-44-STTP-3	44.0	8.40E-01	6.67E-03	3.25E-03
11-48-STTP-3	48.0	8.51E-01	8.06E-03	3.11E-03
12-52-STTP-3	52.0	8.45E-01	8.75E-03	3.11E-03
13-56-STTP-3	56.5	8.92E-01	8.17E-03	4.09E-03
14-60-STTP-3	60.5	8.62E-01	6.67E-03	3.51E-03
15-64-STTP-3	64.0	8.41E-01	7.82E-03	3.49E-03
16-68-STTP-3	68.0	8.65E-01	6.81E-03	3.42E-03
17-72-STTP-3	72.0	8.47E-01	8.18E-03	3.40E-03
18-76-STTP-3	76.3	8.40E-01	7.58E-03	3.64E-03
19-80-STTP-3	80.5	8.53E-01	6.80E-03	3.24E-03
20-84-STTP-3	84.5	8.53E-01	7.52E-03	2.83E-03
21-88-STTP-3	88.0	8.44E-01	9.26E-03	2.67E-03
22-92-STTP-3	92.0	8.62E-01	9.80E-03	3.56E-03
A-93.5-STTP-3	93.5	5.06E-01	6.89E-01	3.58E-03

Table G, Contined.

Sample ID	Time (h)	Pt (mg/L)	Hg (mg/L)	Pb (mg/L)
0-0-STTP-3	0.0	1.11E-02	1.49E-01	3.55E+00
1-8-STTP-3	8.8	< 1.82E-03	< 2.45E-03	1.69E+00
2-12-STTP-3	12.0	< 1.82E-03	< 2.45E-02	2.03E+00
3-16-STTP-3	16.0	8.89E-03	8.59E-02	1.51E+00
4-20-STTP-3	20.0	9.91E-03	3.60E-02	1.36E+00
5-24-STTP-3	24.0	9.72E-03	3.51E-02	1.39E+00
6-28-STTP-3	28.3	7.16E-03	2.17E-02	1.42E+00
7-32-STTP-3	32.3	6.66E-03	2.14E-02	1.38E+00
8-36-STTP-3	36.0	9.92E-03	3.56E-02	1.59E+00
9-40-STTP-3	40.0	8.96E-03	3.68E-02	1.65E+00
10-44-STTP-3	44.0	1.07E-02	3.63E-02	1.81E+00
11-48-STTP-3	48.0	1.24E-02	3.64E-02	1.52E+00
12-52-STTP-3	52.0	1.08E-02	3.49E-02	1.67E+00
13-56-STTP-3	56.5	1.22E-02	3.78E-02	1.64E+00
14-60-STTP-3	60.5	1.09E-02	3.59E-02	1.39E+00
15-64-STTP-3	64.0	7.28E-03	3.68E-02	1.64E+00
16-68-STTP-3	68.0	1.12E-02	3.69E-02	1.82E+00
17-72-STTP-3	72.0	1.02E-02	3.64E-02	1.78E+00
18-76-STTP-3	76.3	9.13E-03	3.30E-02	1.83E+00
19-80-STTP-3	80.5	1.06E-02	3.62E-02	1.66E+00
20-84-STTP-3	84.5	1.15E-02	3.69E-02	1.74E+00
21-88-STTP-3	88.0	1.24E-02	3.51E-02	1.79E+00
22-92-STTP-3	92.0	1.21E-02	3.99E-02	1.85E+00
A-93.5-STTP-3	93.5	1.24E-02	3.20E-02	< 5.52E-05

Table G, Continued.

Sample ID	Time (h)	U-233 (mg/L)	U-235 (mg/L)	U-238 (mg/L)
0-0-STTP-3	0.0	3.19E-03	1.70E-01	3.55E+00
1-8-STTP-3	8.8	< 1.70E-03	< 1.70E-03	1.53E+00
2-12-STTP-3	12.0	< 1.70E-03	< 1.70E-03	1.55E+00
3-16-STTP-3	16.0	2.32E-03	9.82E-02	1.67E+00
4-20-STTP-3	20.0	3.10E-03	1.00E-01	1.63E+00
5-24-STTP-3	24.0	2.04E-03	9.81E-02	1.66E+00
6-28-STTP-3	28.3	1.69E-03	2.23E-02	1.55E-03
7-32-STTP-3	32.3	1.71E-03	2.12E-02	1.74E-03
8-36-STTP-3	36.0	1.72E-03	1.12E-01	1.51E+00
9-40-STTP-3	40.0	1.91E-03	1.07E-01	1.50E+00
10-44-STTP-3	44.0	1.83E-03	1.10E-01	1.52E+00
11-48-STTP-3	48.0	1.82E-03	1.10E-01	1.52E+00
12-52-STTP-3	52.0	1.82E-03	1.10E-01	1.58E+00
13-56-STTP-3	56.5	2.55E-03	1.17E-01	1.60E+00
14-60-STTP-3	60.5	1.86E-03	1.05E-01	1.49E+00
15-64-STTP-3	64.0	3.17E-03	9.30E-02	1.19E+00
16-68-STTP-3	68.0	2.57E-03	8.29E-02	1.22E+00
17-72-STTP-3	72.0	< 1.70E-05	8.63E-02	1.25E+00
18-76-STTP-3	76.3	1.91E-03	9.98E-02	1.36E+00
19-80-STTP-3	80.5	2.17E-03	9.68E-02	1.36E+00
20-84-STTP-3	84.5	1.94E-03	9.91E-02	1.37E+00
21-88-STTP-3	88.0	2.42E-03	9.93E-02	1.43E+00
22-92-STTP-3	92.0	1.67E-03	1.07E-01	1.43E+00
A-93.5-STTP-3	93.5	2.01E-03	8.81E-02	1.48E+00